WADC TECHNICAL REPORT 54-524
PART 2

REDUCTION OF DRAG DUE TO LIFT AT SUPERSONIC SPEEDS

E. W. GRAHAM
P. A. LAGERSTROM
B. J. BEANE
R. M. LICHER
A. M. RODRIGUEZ

DOUGLAS AIRCRAFT COMPANY

AUGUST 1954

AERONAUTICAL RESEARCH LABORATORY
CONTRACT No. AF 33(616)-2170
PROJECT No. 1366

WRIGHT AIR DEVELOPMENT CENTER
AIR RESEARCH AND DEVELOPMENT COMMAND
UNITED STATES AIR FORCE
WRIGHT-PATTERSON AIR FORCE BASE, OHIO

Carpenter Litho & Prtg. Co., Springfield, O.
100 - 3 May 1955

FOREWORD

This report was prepared by the Santa Monica Division of the Douglas Aircraft Company, Inc., under Contract No. AF 33(616)-2170, for the Wright Air Development Center. The authors of this report are Messrs. E. W. Graham, P. A. Lagerstrom, B. J. Beane, R. M. Licher, and A. M. Rodriguez. The work was accomplished under Task No. 70166, titled, "Supersonic Wing Drag Reduction". Captain D. T. Barish and Mr. Fred L. Daum, both of the WADC Aeronautical Research Laboratory, served as Task Scientists.

This is a brief summary report aimed at presenting physical explanations of the complex mathematical theoretical results contained in Part I of this same report, which deals with the reduction of supersonic wing drag through the proper distribution of wing camber and through the application of the "supersonic-biplane" concept.

ABSTRACT

This report is a summary of WADC TR 54-524 Part II which describes a theoretical study into methods of reducing the supersonic drag of wings of the type used in missile design. The reduction of drag due to lift through the use of twist and camber in monoplanes was given special emphasis. Biplanes and other wing systems were also investigated for possible drag reduction or other advantages. These studies showed that it was not possible to develop methods for rapid design of minimum drag wings within the very restrictive manhour limitations applying to this work. But other results applicable to the aerodynamic design of supersonic vehicles were obtained and these are:

At supersonic speeds twist and camber can be used to reduce the drag due to lift of monoplanes. For certain planforms camber alone is needed. The reduction in drag due to lift is largest for low supersonic speeds, for low aspect ratios, and is larger for delta or diamond planforms than rectangular planforms of the same aspect ratio.

Various methods for drag minimization were considered. The general integral equation defining optimum camber and twist was derived but not solved. For purposes of calculation approximate methods were used.

From the study of lift distributed throughout a prescribed volume it was found that such distributuions show potential for greater reductions in drag due to lift than do the best monoplanes contained within the volume. This indicates the possibility that multiplanes may have lower drag due to lift than monoplanes.

Biplanes with wings not in each other's Mach cones show a possible structural weight advantage over monoplanes.

PUBLICATION REVIEW

This report has been reviewed and is approved.

FOR THE COMMANDER:

Leslie B. Williams

LESLIE B. WILLIAMS
Colonel, USAF
Chief, Aeronautical Research Laboratory
Directorate of Research

CONTENTS

CHAPTER I

INTRODUCTION

INTRODUCTION

Drag is the dissipative force acting on an airplane. A large weight of fuel is needed to provide the energy spent by the drag and large, heavy powerplants are needed to convert the fuel's energy into useful work. Limitations on speed, range, and other performance characteristics are imposed by drag. For these reasons, the development of methods for drag reduction is of great importance in the advancement of aircraft performance. While this has always been true, it is particularly so for present supersonic airplane configurations because the drag of these is too great to allow economical flight over ranges of useful length. In an effort to improve this situation, an exploration of several means for reducing drag due to lift at supersonic speeds was undertaken. These studies are reported here.

Several questions arise in interpreting work in the field of drag reduction. These are:

1. What is the magnitude of the improvement resulting from drag reduction? By what percentage can performance be increased for each percent reduction of drag?
2. What are the magnitudes of the various components of the drag? What elements of the drag are so large that improvement in them may result in large total drag savings?

The remarks that follow are intended to indicate the answers to these questions.

The relationship between the magnitude of reduction in an element of the drag and the resulting performance change of an airplane still in the design stage may be a complex one. In a simple case, where the change in

the drag is the only change, and where range is the only performance characteristic considered, the following argument is often used. An airplane with mean drag D when flying a distance R expends energy DR. This energy is obtained from burning a quantity W_F of fuel with heat content H in a propulsion system of overall efficiency η_o. It then follows that $D \cdot R = H\eta_o W_F$. For an airplane with given types of fuel and powerplant (which fix H and η_o) and for constant range, $dW_F/W_F = dD/D$. A 10% drag decrease therefore leads to a fuel weight saving (and an increase in payload, W_{PL}) which is 10% of the fuel weight. If the drag change is also assumed to allow a proportional reduction in powerplant weight, W_{PP}, then for constant initial gross weight $dW_{PL}/W_{PL} = -(dD/D) \cdot [(W_{PP}+W_F)/W_{PL}]$. To a rough approximation the powerplant plus fuel weight is half the gross weight and the payload is a sixth the gross weight so that $dW_{PL}/W_{PL} = -3dD/D$. Thus, in this example, a 10% drag reduction corresponds to a 30% payload increase. This is of great importance to the utility of the airplane.

In the more general situation the estimation of the effect of drag reduction on performance is not so simple. The alteration in geometry necessary to achieve the original change in drag may lead to other drag effects, favorable or not. It may affect, favorably or otherwise, the various components of the gross weight, the maximum lift, the stalling characteristics, the handling qualities, the stability, and the control and maneuverability. It may influence the choice of powerplant and fuel types and the engine size and weight. Furthermore, these effects will vary with the mission of the airplane. Thus, a change in an important ingredient of the design necessitates re-examination of all other ingredients and the creation of a new recipe. Despite these complications the drag reduction often is

favorably reflected as a performance improvement. For example, the drag reduction could affect the design as follows. The lowered drag would make it possible to use engines of smaller thrust and weight. This would lead to a smaller, lighter, lower drag fuselage or nacelles. In turn, this would allow a smaller wing and landing gear. Additional drag improvement would arise, and the engine size again would be favorably affected. The process would converge and a much improved airplane would result. Although only the range problem has been discussed, consideration of maximum speed, ceiling, etc., similarly would show the important influence of drag reduction.

At the present time drag reduction is crucially needed to allow supersonic flight of even low efficiency. Major drag reduction at supersonic speeds is needed before efficient, long range supersonic flight can occur.

With regard to the second question posed - the drag elements so large that improvement in them could result in large drag savings - Fig. 1 is illuminating. At subsonic speeds it is possible to design wings with maximum lift:drag ratios in excess of 40, and complete airplanes with $(L/D)_{max}$ of almost 20. Fig. 1 shows that at supersonic speeds the L/D for only the wing, even before allowance is made for wave drag due to thickness, is roughly half that for complete efficient aircraft at subsonic speeds. Although at the lower supersonic Mach numbers highly swept leading edges may be used to alleviate this situation, the point illustrated is that the shaping of the wing to minimize the drag due to lift is of great importance. It is this drag that is most responsible for the degraded performance of the supersonic wing.

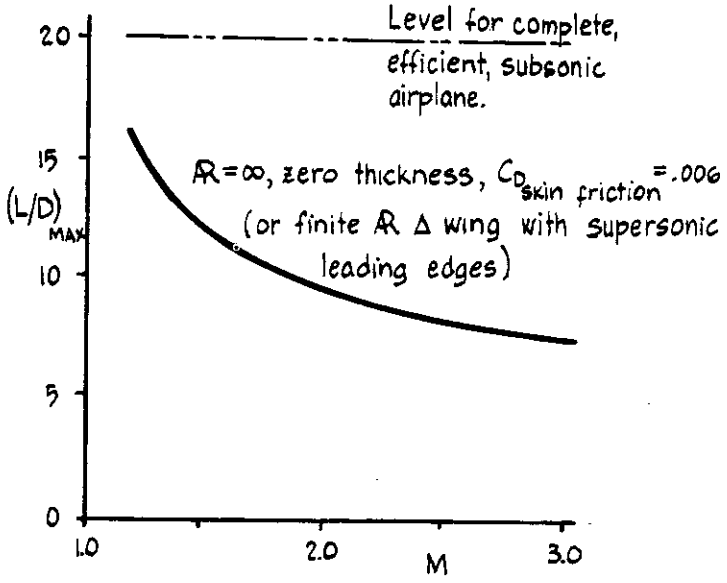

Fig. 1

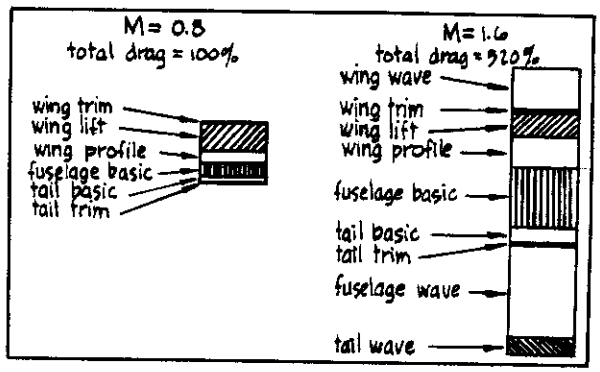

Ref. "Straight Wing or Delta for High Speed Flight" by C.L. Johnson, Aviation Age, Dec. 1953, Vol.20, No.6.

Fig. 2

A second area in which the drag penalties now are large is illustrated by Fig. 2, i.e., the wave drags associated with the thickness distributions of the fuselage and the lifting surfaces. The minimization of these drags through better shaping or through the discovery and application of favorable interference (not considered in this report) is also of great importance. To achieve large improvements in the drag due to lift and the wave drag due to thickness, it may be necessary to resort to unconventional configurations.

The subsequent chapters are a discussion of several topics relating to means for the reduction of drag due to lift at supersonic speeds. Except as related to the overall problem, the topics are independent of one another, one chapter being devoted to each topic, and each chapter being written as an independent entity.

CHAPTER II

DRAG DUE TO LIFT OF PLANAR WINGS OF FIXED PLANFORM

by

P. A. Lagerstrom
A. M. Rodriguez
R. M. Licher

1. SUMMARY

For a few planforms the angle of attack distribution required for minimum drag is already known. Also known are some general theorems regarding minimum drag and some methods for obtaining the required shape. Here many of these concepts and theorems are extended for a restricted class of loadings. A relation is found for the interference drag between any loading within this class and the optimum loading within the class. The integral equation for the optimum among all possible loadings within the class is found.

Specific calculations are made for the sonic edge diamond planform and for the rectangular planform wing. The loading and camber distribution for the former is calculated by a method of successive orthogonalization of loadings up to a distribution composed of six orthogonal loadings. The optimum corresponding to twelve component loadings is found by solving a set of linear equations arising from the minimization of D/L^2 to give the intensity of the component loadings. It is found that the major drag reduction results from the α-distributions varying with x^3 and xy^2 in optimal combination, x and y being distances in the chordwise and spanwise directions, respectively.

From a study of the properties of rectangular wings it is concluded that the drag due to lift of a rectangular wing may be decreased by a spanwise variation in camber, in particular by a decrease in camber in the middle section. Some simple types of spanwise variation are investigated and a lower bound for the drag is calculated.

The calculated results indicate that substantial savings in drag at a given lift can be achieved only for low reduced aspect ratios. With such geometries wing-body interference becomes important and must be accounted for.

2. INTRODUCTION

The problem to be discussed in the present chapter is that of minimizing the drag due to lift for a wing of given planform in supersonic flow.

The analysis will be based on the customary assumptions of linearized theory. Hence, in particular, in studying the drag due to lift one may assume that the wing has zero thickness. The problem to be solved is then to find a distribution of local angle of attack for a wing of given lift and planform such that the resulting drag is as small as possible.

In subsonic flow this problem is essentially solved. For supersonic flow general methods have been developed in particular by R. T. Jones[1] and by E. W. Graham[2]. The methods of Graham have been developed further in Ref. 3. The references cited contain several general theorems regarding and methods for obtaining minimum drag. These methods have also been applied to specific planforms. Jones[4] has found that for wings of elliptic planform a constant pressure distribution gives minimum drag. He also showed[1] that in the limit of very low aspect ratio the minimum drag of a wing is obtained when both the spanwise and chordwise lift distribution is elliptical. Calculations have also been carried out to find angle-of-attack-distributions which give lower drag than, say, a constant distribution without actually giving the absolute drag minimum. Examples of such computations, based essentially on the method of Graham, are to be found in Ref. 5 and 6.

S. H. Tsien[7] found the minimum drag of a narrow delta wing for conical distributions of angle of attack. Sedney[10] and Rott[8], independently and by different methods, found the minimum drag of a rectangular wing subject to the restriction that the angle of attack has no spanwise variation.

The present chapter is concerned both with general theorems and calculations for specific planforms. The work is mainly based on Ref. 3. Space does not permit a repetition of the definitions, theorems and discussion given there. Only a very brief review of some parts of Ref. 3, etc., is given in Section 3 where some additional concepts and theorems also are introduced. For further details the reader is referred to Ref. 3.

The results of specific calculations are presented for two examples. In Section 4 the wing of diamond planform with sonic edges is discussed. This example illustrates the influence of taper alone. The wing of rectangular planform is discussed in Section 5. In this example there is no influence of taper, of course, and the effects are due solely to the tips.

The problem of minimum drag for the diamond planform is solved in the following sense:

> A comparatively simple procedure for successively lowering the drag at fixed lift is described. This procedure is carried out analytically and numerically and an angle of attack distribution is found for which the drag probably differs from the minimum drag by only a fraction of a percent.

The methods used may be extended to other planforms, in particular to that of a delta wing with sonic edges.

The results for the rectangular wing are less complete than those for the diamond planform case. However, some reasonable drag reductions are obtained and it is believed that the drag obtained is not appreciably above the minimum. Also, a lower bound for the drag is derived. The value obtained for this bound may be appreciably below the actual minimum. The method used is very simple and general, however, and possibly may be refined further.

3. GENERAL DISCUSSION

The notation, concepts and theorems of Ref. 3 will be used as a basis for the subsequent discussion in the present chapter. Only the most essential parts of Ref. 3 will be reviewed below. In addition some extensions will be given.

The coordinates are chosen so that z=0 is the plane of the wing and the free stream velocity of magnitude U is directed in the positive x-direction. The Mach number will be taken to be $\sqrt{2}$. $\alpha(x,y)$, which denotes the local angle of attack distribution, will, because of the assumption of zero thickness, have the same value at corresponding points on the lower and upper surfaces of the wing. For convenience $p(x,y)$ will denote the difference in pressure between lower and upper surfaces of the wing, i.e., it is the local lift. By the formulas of linearized wing theory a given $\alpha(x,y)$ determines $p(x,y)$ and vice versa. An angle of attack distribution and its associated lift distribution will be referred to as a load distribution or a loading. Since α and p determine each other, only one of them need be indicated. Two loadings α_1 and α_2 are said to be of the same type if $\alpha_1 = c\alpha_2$, c=constant. For integration of any quantity $f(x,y)$ over the wing planform S the following abbreviated notation will be used:

$$\int_S f(x,y)\,dx\,dy = \int f\,dS = \int f \tag{3-1}$$

With this notation

$$LIFT = L = \int p \tag{3-2a}$$

$$DRAG = D = \int p\alpha \tag{3-2b}$$

The ratio

$$d = \frac{D}{L^2} \tag{3-3}$$

is the same for all distributions of the same type. The basic problem is to find a distribution, or rather type of distribution, which minimizes d. It will be convenient to introduce a notation for the inverse of d. This inverse will be given the non-dimensional form

$$\ell = \frac{1}{q_\infty S d} = \frac{L^2}{D q_\infty S} = \frac{C_L^2}{C_D} \tag{3-4}$$

where S=wing area, $q_\infty = \frac{1}{2}\rho U^2$ If α is constant, i.e, if the wing is a flat plate, then D=αL (leading edge suction is neglected, see Ref. 3), and the corresponding d and ℓ will be denoted by the subscript "f":

$$d_f = \alpha/L, \qquad \ell_f = dC_L/d\alpha \tag{3-5}$$

An optimal loading, that is a loading with minimum drag, has a maximum ℓ and a minimum d. The drag reduction achieved by any loading may be measured conveniently by comparing it with the flat plate loading of the same planform, that is, one may form $\frac{d}{d_f}$ or its inverse $\frac{\ell}{\ell_f}$. Another natural reference value is the two-dimensional optimum. This optimum is achieved by a flat plate loading and is

$$\ell_{2\,DIM} = (dC_L/d\alpha)_{2\,DIM} = 4 \tag{3-6}$$

If two loadings α_1 and α_2 have drag D_1 and D_2 respectively the inner product or interference drag between the loadings will be denoted by (α_1,α_2) or D_{12} and defined by

$$D_{12} = (\alpha_1,\alpha_2) = \int(p_1\alpha_2 + p_2\alpha_1) = D_{21} = (\alpha_2,\alpha_1) \tag{3-7}$$

The drag, D, of the loading $(\alpha_1+\alpha_2)$ is then

$$D = D_1 + D_2 + D_{12} \tag{3-8}$$

where $D_1 = \frac{1}{2}(\alpha_1,\alpha_1)$ AND $D_2 = \frac{1}{2}(\alpha_2,\alpha_2)$

Two loadings are said to be orthogonal if they have no interference drag, that is $D_{12}=0$.

Many of the concepts and theorems of Ref. 3 may be extended to a restricted class of loadings. A collection, C, of loadings will be called a restricted class if it does not include all possible loadings but still is closed in the following sense:

> if the loadings α_i are in C and if λ_i are constants then $\sum \lambda_i \alpha_i$ is a loading in C whenever the series converges.

Important examples of restricted classes of loadings are the following. For planforms that are symmetric about the spanwise y-axis, loadings that are odd in x, i.e., $\alpha(x,y)= -\alpha(-x,y)$ form a restricted class. If α_1 and α_2 belong to this class the expression for the interference drag may be simplified to (cf. Ref. 3, Eq. 30)

$$D_{12} = 2\int \alpha_1 p_2 = 2\int \alpha_2 p_1 \tag{3-9}$$

Another example is the class of loadings on a conical planform such that α is constant along conical rays.

Many of the theorems of Ref. 3 are still valid for restricted classes of loadings. So for example one may form a complete orthogonal set α_i within a given restricted class C so that any other loading α in C may be expressed as

$$\alpha = \sum a_i \alpha_i \tag{3-10a}$$

$$(\alpha_i, \alpha_j) = 0 \qquad \text{FOR } i \neq j \tag{3-10b}$$

$$(\alpha_i, \alpha_i) = 2D_i \qquad \text{WHERE } D_i = \text{DRAG OF } \alpha_i \tag{3-10c}$$

$$a_i = \frac{(\alpha, \alpha_i)}{2D_i} \tag{3-10d}$$

$$\int p_i = L_i = \text{LIFT OF } \alpha_i \tag{3-10e}$$

$$\ell_i = \frac{L_i^2}{D_i q S} \tag{3-10f}$$

The optimal loading α_{opt} relative to the class C then has the properties (L_{opt} and D_{opt} are the lift and drag of α_{opt} respectively)

$$\alpha_{opt} = \frac{D_{opt}}{L_{opt}} \sum \frac{L_K}{D_K} \alpha_K \tag{3-11a}$$

$$\alpha_{opt} = \frac{1}{\sum \frac{1}{d_K}} \tag{3-11b}$$

$$\ell_{opt} = \sum \ell_K \tag{3-11c}$$

This corresponds to Theorem 3 of Ref. 3. Parts of Theorem 6 of Ref. 3 may also be generalized. We first note that if α is in C then* $\tilde{\alpha} = -\alpha$ is in C. However, it is not true in general that $\bar{\alpha}$ is in C. The optimum in C in forward flow may be decomposed into a sum of two orthogonal loadings $(\alpha_{opt})_{fwd} = \alpha_A + \alpha_B$ where α_A is a constant. It is thereby assumed that α_A, and hence α_B, is in C.

Consider now reversed flow past the angle-of-attack distribution contained in C. It is then easily proved (cf. Theorem 6 and Eq. 28 and 29 of Ref. 3), that $(\alpha_{opt})_{rev} = \alpha_A - \alpha_B$. However, unless $(\alpha_{opt})_{fwd}$ is the absolute optimum among all loadings of the given planform, the pressure distributions corresponding to $(\alpha_{opt})_{fwd}$ and $(\alpha_{opt})_{rev}$ must be different. If they are identical, i.e., $(p_{opt})_{fwd} = (p_{opt})_{rev}$, the sum of the α's corresponding to this pressure distribution in forward and reverse flow is $(\alpha_A + \alpha_B) + (\alpha_A - \alpha_B) = 2\alpha_A$ = constant. Hence the loading would be the absolute optimum by Jones' criterion. To summarize:

If $(\alpha_{opt})_{fwd}$ is the optimum in forward flow of a restricted class C which contains the flat plate loadings then

$$(\alpha_{opt})_{FWD} = \alpha_A + \alpha_B \tag{3-12a}$$

$$(\alpha_{opt})_{REV} = \alpha_A - \alpha_B \tag{3-12b}$$

*The notation is that of Ref. 3 where $\tilde{\alpha}$ denotes the angle of attack distribution for a wing of fixed geometry in reverse flow and $\bar{\alpha}$ is the angle of attack distribution for a wing in which the total lift (and planform geometry) is maintained fixed in reverse flow.

where α_A = constant and $(\alpha_A, \alpha_B) = 0$

Furthermore

$$(p_{opt})_{fwd} = (p_{opt})_{rev} \text{ implies } \alpha_{opt} = \text{absolute optimum} \tag{3-12c}$$

Finally α_B must be the optimum among the loadings in C which are orthogonal to the flat plate.

If in addition the planform is symmetrical about the y-axis and $\alpha(-x,y)$ is in C whenever $\alpha(x,y)$ is in C, then

$$\alpha_B(-x,y) = -\alpha_B(x,y) \tag{3-13}$$

This is proved in the same way as Theorem 8c of Ref. 3.

Finally a relation and an associated integral equation will be derived which were not stated explicitly in Ref. 3. Consider a restricted class C with optimum α_{opt}. Let α be a loading in C with lift L. Then it may be shown that

$$(\alpha_{opt}, \alpha) = \frac{2 D_{opt}}{L_{opt}} L \tag{3-14}$$

This is proved as follows. Make α the first term in a complete orthogonal set (α_i) and express α_{opt} as above (Eq. 3-11a). Then form the inner product (α_{opt}, α). Since by construction $(\alpha, \alpha_i)=0$ for $i \geq 2$ it follows from Eq. 3-11a

$$(\alpha_{opt}, \alpha) = \frac{D_{opt}}{L_{opt}} \frac{L}{D} (\alpha, \alpha) = \frac{D_{opt}}{L_{opt}} \frac{L}{D} 2D$$

which proves Eq. 3-14.

From Eq. 3-12 one may derive an integral equation for the optimal loading. On the wing consider a rectangular element lying between x and $x+\Delta x$ and between y and $y+\Delta y$, with an angle of attack, α, such that $\alpha \cdot \Delta x \cdot \Delta y = 1$, and let the remainder of the wing be at zero angle of attack.

The limiting singular deflection as Δx and Δy tend to zero will be referred to as a unit deflection at the point $P=(x,y)$. The angle of attack distribution may then also be written with the aid of a Dirac delta function $\alpha(Q)=\delta(P-Q)=\delta(\xi-x, \eta-y)$ where $Q=(\xi, \eta)$ is an arbitrary point on the wing. We define a Green's function G by

$$G(P;Q)= G(x,y;\xi,\eta) = \text{local lift at Q due to unit deflection at P} \qquad (3\text{-}15a)$$

and

$$G_r(P;Q)=G_r(x,y;\xi,\eta) = \text{local lift at Q due to unit deflection at P in reverse flow} \qquad (3\text{-}15b)$$

Let P and Q be two fixed points and R be a variable point. Consider a unit deflection at P in forward flow and a unit deflection at Q in reverse flow. The reciprocity theorem (see Ref. 3 Eq. 5 and references given there) yields

$$\int \delta(P-R)G_r(Q;R)dR = \int \delta(Q-R)G(P;R)dR$$

or

$$G_r(Q;P) = G(P;Q) \qquad (3\text{-}16)$$

Note that G(P;Q) is zero except if Q is in the downstream Mach cone of P. G is singular along the edges of this Mach cone (see Ref. 9, p.18 ff). If there is no edge interference G depends on the coordinate difference $Q-P=(\xi-x, \eta-y)$ only.

From the reciprocity theorem and Eq. 3-14 it also follows that if $\alpha(Q)=\delta(P-Q)$ then

$$\int \alpha(Q)p_{opt}(Q)dQ = p_{opt}(P) = \int \alpha_{opt}(Q)G_r(P;Q)dQ = \int \alpha_{opt}(Q)G(Q;P)dQ \qquad (3\text{-}17)$$

If now Eq. 3-14 is applied to $\alpha=\delta(P-Q)$ and use is made of Eq. 3-17 one obtains

$$\int \alpha_{opt}(Q)\left[G(P;Q)+G(Q;P)\right]dQ = \frac{2D_{opt}}{L_{opt}}\int G(P;Q)dQ \qquad (3\text{-}18)$$

Since G(P;Q) may be computed by standard methods of wing theory, Eq. 3-18 is an integral equation for α_{opt}. It may also be derived as follows:

One has

$$D_{opt} = \iint \alpha_{opt}(P)\alpha_{opt}(Q)G(P;Q)\,dP\,dQ \tag{3-19a}$$

$$L_{opt} = \iint \alpha_{opt}(P)G(P;Q)\,dP\,dQ \tag{3-19b}$$

Furthermore

$$D_{opt} + \lambda L_{opt} = \text{MINIMUM} \tag{3-20}$$

where λ is a Lagrangian multiplier. By an elementary method of the calculus of variation one may derive Eq. 3-17 from Eq. 3-18. It is thereby easily seen that $\lambda = -\frac{2D_{opt}}{L_{opt}}$ (cf. the derivation of Eq. 5-6).

Eq. 3-18 is actually the integral equation for the optimum among all possible loadings. Corresponding equations for restricted classes of loadings are easily derived the same way, either from Eq. 3-14 or by the variational method. Examples will be given in discussion of rectangular wings (Section 5).

4. OPTIMAL LOADING FOR THE DIAMOND PLANFORM

To illustrate the drag reduction methods outlined in the previous section, a diamond shaped planform with sonic leading and trailing edges will now be discussed. This planform shape was chosen because of simplicity in calculating the local lift distribution, total lift and drag of and the interference drags between certain loadings whose angle of attack distributions are polynomials with simple properties.

The coordinate system chosen for the diamond planform is shown in Fig.4-1. The local lift distribution is computed from the angle of attack distribution by means of the relation

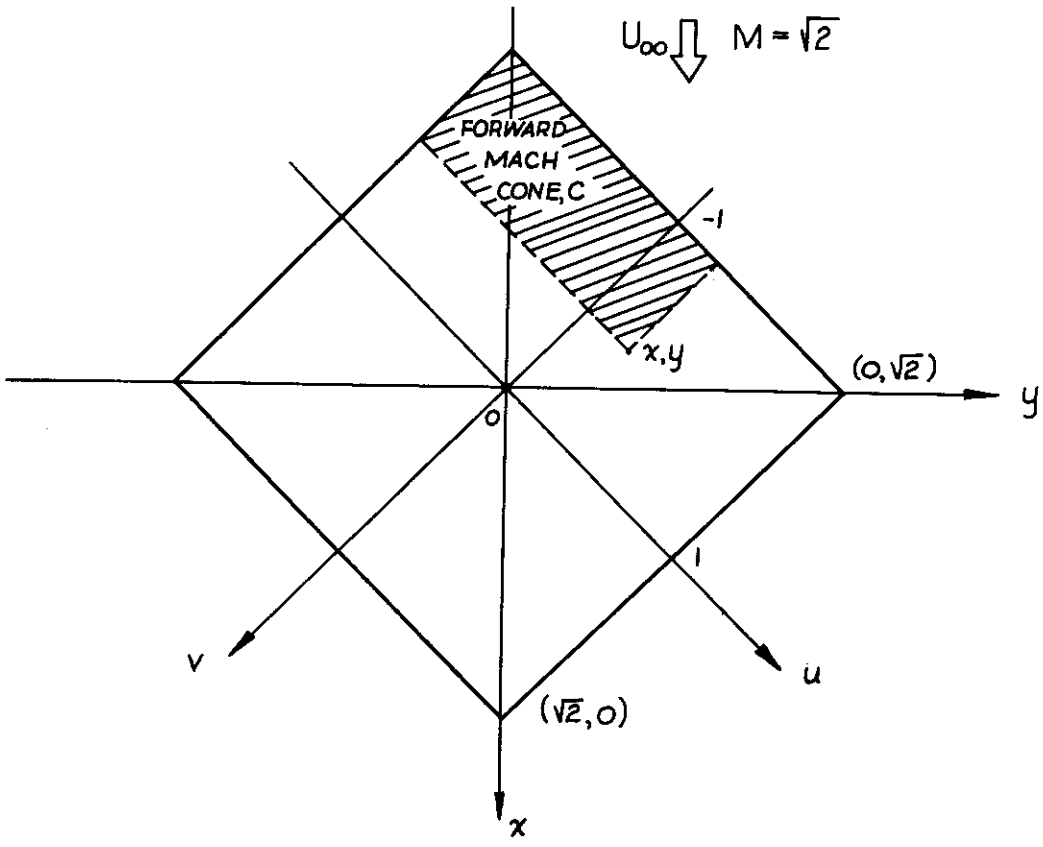

Figure 4-1

$$p(x,y) = \frac{4q}{\pi} \frac{\partial}{\partial x} \iint_C \frac{a(\xi,\eta)\, d\xi d\eta}{\sqrt{(x-\xi)^2-(y-\eta)^2}} \tag{4-1}$$

from linearized flow theory.

By a rotation of the coordinates through 90°, Mach coordinates are introduced

$$x = \frac{1}{\sqrt{2}}(u+v) \quad , \quad y = \frac{1}{\sqrt{2}}(u-v)$$
$$\xi = \frac{1}{\sqrt{2}}(\mu+\upsilon) \quad , \quad \eta = \frac{1}{\sqrt{2}}(\mu-\upsilon) \tag{4-2}$$

Eq. 4-1 then reduces to the simpler form

$$p(u,v) = \frac{2q}{\pi}\left(\frac{\partial}{\partial u} + \frac{\partial}{\partial v}\right) \int_{-1}^{u} \int_{-1}^{v} \frac{a(\mu,\upsilon)\, d\mu d\upsilon}{\sqrt{(u-\mu)(v-\upsilon)}} \tag{4-3}$$

The calculations are further simplified by letting

$$u = -\cos\Theta, \quad \mu = -\cos\phi, \quad v = -\cos\bar{\Theta}, \quad \upsilon = -\cos\bar{\Phi} \tag{4-4}$$

Eq. 4-3 then becomes

$$p(\Theta,\bar{\Theta}) = \frac{2q}{\pi \sin\Theta \sin\bar{\Theta}}\left(\sin\bar{\Theta}\frac{\partial}{\partial\Theta} + \sin\Theta\frac{\partial}{\partial\bar{\Theta}}\right) \int_0^{\Theta} \int_0^{\bar{\Theta}} \frac{a(-\cos\phi,-\cos\bar{\phi})\sin\phi\sin\bar{\phi}\, d\phi\, d\bar{\phi}}{\sqrt{(\cos\phi-\cos\Theta)(\cos\bar{\phi}-\cos\bar{\Theta})}} \tag{4-5}$$

According to Ref. 3 Eq. 28, the optimal angle of attack is a sum of two orthogonal loadings

$$\alpha_{opt} = \alpha_A + \alpha_B$$

where α_A is the flat plate loading, α_A=1, and α_B is anti-symmetrical in x and symmetrical in y. In the (u, v) coordinates this symmetry is expressed as

$$\alpha_B(u,v) = \alpha_B(v,u) = -\alpha_B(-v,-u) \tag{4-6}$$

Now, any finite continuous angle-of-attack distribution with the symmetry properties of Eq. 4-6 may be approximated uniformly by a finite sum of loadings of the form

$$\alpha_{m,n} = P_{2m}(u)\, P_{2n+1}(v) + P_{2n+1}(u)\, P_{2m}(v) \tag{4-7}$$

where the P's are Legendre polynomials. The corresponding pressure distribution can then be readily calculated with the aid of the relation

$$\int_0^{\theta} \frac{P_n(\cos\phi)\sin\phi\, d\phi}{\sqrt{\cos\phi - \cos\theta}} = \frac{2\sqrt{2}}{(2n+1)} \sin(2n+1)\frac{\theta}{2} \tag{4-8}$$

Writing Eq. 4-7 in the θ, $\bar{\theta}$ coordinates and denoting $\frac{2q}{\pi}$ by K one obtains

$$\alpha_{m,n}(\theta,\bar{\theta}) = -\left[P_{2m}(\cos\theta)P_{2n+1}(\cos\bar{\theta}) + P_{2n+1}(\cos\theta)\, P_{2m}(\cos\bar{\theta})\right] \tag{4-9}$$

$$P_{m,n}(\theta,\bar{\theta}) = \frac{-4K}{\sin\theta \sin\bar{\theta}\,(4m+1)(4n+3)}\left[\Psi \sin\bar{\theta} + \Phi \sin\theta\right] \tag{4-10}$$

WHERE

$$\Psi = (4m+1)\cos(4m+1)\frac{\theta}{2}\sin(4n+3)\frac{\bar{\theta}}{2} + (4n+3)\cos(4n+3)\frac{\theta}{2}\sin(4m+1)\frac{\bar{\theta}}{2}$$

$$\Phi = (4n+3)\sin(4m+1)\frac{\theta}{2}\cos(4n+3)\frac{\bar{\theta}}{2} + (4m+1)\sin(4n+3)\frac{\theta}{2}\cos(4m+1)\frac{\bar{\theta}}{2}$$

The total lift of $\alpha_{m,n}$ is obtained by integrating Eq. 4-10 over the planform. Thus

$$L(\alpha_{m,n}) = \frac{-64K}{(4m+1)(4n+3)}\left[\frac{1}{(4n+1)(4n+5)} + \frac{1}{(4m-1)(4m+3)}\right] \tag{4-11}$$

The interference drag between any two loadings $\alpha_{m,n}$ and $\alpha_{p,q}$ is given by

$$D_{m,n;\,p,q} = (\alpha_{m,n}, \alpha_{p,q}) = (\alpha_{p,q}, \alpha_{m,n}) = D_{p,q;\,m,n}$$

$$= \frac{1}{2}\int_S (\alpha_{m,n}\, p_{p,q} + \alpha_{p,q}\, p_{m,n})\, dS$$

$$= \int \alpha_{m,n}\, p_{p,q}\, dS \qquad \text{(FROM PLAN FORM SYMMETRY AND Eq 3-6 OR 2-9)}$$

$$= -2\int_0^{\pi}\int_0^{\pi} P_{2m}(\cos\theta)\, P_{2n+1}(\cos\bar{\theta})\, p_{p,q}(\theta,\bar{\theta})\, \sin\theta \sin\bar{\theta}\, d\theta\, d\bar{\theta}$$

$$= \frac{8K}{(4p+1)(4q+3)}\Big\{(4p+1)\Big[A_{2m,2p}B_{2n+1,2q+1} + A_{2n+1,2p}B_{2m,2q+1}\Big]$$

$$+(4q+3)\Big[A_{2n+1,2p}B_{2m,2q+1} + A_{2m,2q+1}B_{2n+1,2p}\Big]\Big\} \qquad (4\text{-}12)$$

where the A's and B's are given by

$$A_{\rho,\sigma} = \int_0^{\pi} P_\rho(\cos\theta)\cos(2\sigma+1)\frac{\theta}{2}\, d\theta \qquad (4\text{-}13)$$

$$B_{\rho,\sigma} = \int_0^{\pi} P_\rho(\cos\theta)\sin(2\sigma+1)\frac{\theta}{2}\, \sin\theta\, d\theta \qquad (4\text{-}14)$$

Although the A's and B's can be computed by direct integration by expanding $P_\rho(\cos\theta)$ in terms of $\cos\rho\theta$, they can be computed more simply by means of the recurrence formula for Legendre polynomials

$$P_\rho(\cos\theta) = \frac{2\rho-1}{\rho}\cos\theta\, P_{\rho-1}(\cos\theta) - \frac{\rho-1}{\rho}\, P_{\rho-2}(\cos\theta) \qquad (4\text{-}15)$$

Noting that

$$\cos(2\sigma+1)\frac{\theta}{2}\cos\theta = \frac{1}{2}\left[\cos(2\sigma+3)\frac{\theta}{2} + \cos(2\sigma-1)\frac{\theta}{2}\right]$$

$$\sin(2\sigma+1)\frac{\theta}{2}\sin\theta = \frac{1}{2}\left[\cos(2\sigma-1)\frac{\theta}{2} - \cos(2\sigma+3)\frac{\theta}{2}\right]$$

the recurrence formula for the A's is given by

$$A_{\rho,\sigma} = \frac{2\rho-1}{2\rho}\left(A_{\rho-1,\sigma+1} + A_{\rho-1,\sigma-1}\right) - \frac{\rho-1}{\rho}A_{\rho-2,\sigma} \qquad (4\text{-}16)$$

The B's can then be computed from the A's

$$B_{\rho,\sigma} = \frac{1}{2}\left(A_{\rho,\sigma-1} - A_{\rho,\sigma+1}\right) \qquad (4\text{-}17)$$

The initial values of the A's for $\rho=0$ and $\rho=1$ are

$$A_{0,\sigma} = (-1)^{\sigma}\frac{2}{2\sigma+1} \qquad (4\text{-}18)$$

$$A_{1,\sigma} = \frac{(-1)^{\sigma+1}2(2\sigma+1)}{(2\sigma+3)(2\sigma-1)} \qquad (4\text{-}19)$$

From these, any $A_{\rho,\sigma}$ can be computed by successive use of the recurrence formula Eq. 4-16. The values of the A's and B's are tabulated in Tables 1 and 2 of the appendix.

The loading with minimum drag corresponds to the optimum linear combination of α-distributions $\alpha_{m,n}$ of the complete set. As an approximation the minimal drag corresponding to a restricted set of $\alpha_{m,n}$'s was found. The drag when the restricted set is composed of 1,2,3,....6,12 distributions has been found and it will be seen that as the restricted set is enlarged the drag converges on a minimum. The following rectangular array of $\alpha_{m,n}$ was chosen:

$$\left\{\begin{array}{cccc} \alpha_{0,0} & \alpha_{0,1} & \alpha_{0,2} & \alpha_{0,3} \\ \alpha_{1,0} & \alpha_{1,1} & \alpha_{1,2} & \alpha_{1,3} \\ \alpha_{2,0} & \alpha_{2,1} & \alpha_{2,2} & \alpha_{2,3} \\ \alpha_{3,0} & \alpha_{3,1} & \alpha_{3,2} & \alpha_{3,3} \end{array}\right\} \qquad (4\text{-}20)$$

The interference drags $(\alpha_{m,n},\alpha_{p,q}) = D_{m,n;p,q}$ were computed for this array and are given in Table 3 of the appendix. The $A_{\rho,\sigma}$ and $B_{\rho,\sigma}$ needed for the computation of the $D_{m,n;p,q}$ according to Eq. 4-12 were taken from Tables 1 and 2. In Table 4 are given the values of $L(\alpha_{m,n})$ which were calculated according to Eq. 4-11. All calculations were made with the aid of a desk calculator.

The following six loadings were considered first:

$$\beta_1 = \alpha_{0,0} \qquad \beta_2 = \alpha_{1,0} \qquad \beta_3 = \alpha_{0,1}$$

$$\beta_4 = \alpha_{1,1} \qquad \beta_5 = \alpha_{2,0} \qquad \beta_6 = \alpha_{2,1}$$

These loadings, β_i , are not orthogonal. By the method of successive orthogonalization described in Ref. 2, a set of orthogonal loadings, $\alpha_0,\alpha_1,\ldots\alpha_6$, may be constructed through linear combinations of the β_i's and the flat plate loading. These loadings, by calculation with a desk calculator, were found to be

$$\begin{aligned}
\alpha_0 &= 1 \\
\alpha_1 &= \beta_1 \\
\alpha_2 &= \beta_2 + 0.066667\beta_1 \\
\alpha_3 &= \beta_3 - 0.415839\beta_2 - 0.226669\beta_1 \\
\alpha_4 &= \beta_4 - 0.039697\beta_3 + 0.156964\beta_2 + 0.039856\beta_1 \\
\alpha_5 &= \beta_5 - 0.346250\beta_4 + 0.147251\beta_3 - 0.277337\beta_2 - 0.041748\beta_1 \\
\alpha_6 &= \beta_6 - 0.165236\beta_5 + 0.239505\beta_4 - 0.036767\beta_3 + 0.139395\beta_2 + 0.024050\beta_1
\end{aligned} \qquad (4\text{-}21)$$

Since the α_i's are orthogonal Eq. 3-10 and Eq. 3-11 may be used to find the lift, drag, and optimum angle of attack distribution. This optimum, in terms of the α_i's, was found to be

$$\alpha_{opt} = 1 + 0.152174\alpha_1 - 0.551776\alpha_2 + 0.503619\alpha_3 - 0.535686\alpha_4 + 0.141534\alpha_5 - 0.555888\alpha_6 \qquad (4\text{-}22)$$

The quantities l_i/l_f were found to be

$$\frac{l_1}{l_f} = 0.020239, \quad \frac{l_2}{l_f} = 0.040636, \quad \frac{l_3}{l_f} = 0.096068$$

$$\frac{l_4}{l_f} = 0.015544, \quad \frac{l_5}{l_f} = 0.000996, \quad \frac{l_6}{l_f} = 0.008724$$

where $$l_f = \frac{L^2}{DqS} = \frac{L}{\alpha qS} = \frac{dC_L}{d\alpha} = 3.3953$$

for the flat plate loading. Using the equation

$$\frac{\Delta D}{D_o} = \frac{\sum \frac{l_i}{l_f}}{1+\sum \frac{l_i}{l_f}} = \text{fractional drag reduction from flat plate loading} \qquad (4\text{-}23)$$

the successive drag reductions obtained by terminating the series Eq. 4-20 successively at α_1, α_2, ..., α_6 over the flat plate drag are given in the table below.

α_{opt} Terminated at	% Drag Reduction From Flat Plate Loading $(100)\Delta D/D$
α_1	1.989
α_2	5.743
α_3	13.569
α_4	14.715
α_5	14.787
α_6	15.416

An indication of the degree of approximation given by Eq. 4-22 to the actual minimum drag loading was obtained by computing the optimum linear combination of all twelve loadings in the array Eq. 4-20 combined with the flat plate α_o=1 and comparing the drag reduction to the drag reduction obtained from the approximation Eq. 4-22. The increasing complication involved in the calculation of additional orthogonal loadings

on a desk calculator was found to be too time consuming. The method of successive orthogonalization was not used to calculate the optimum angle of attack including the remaining six loadings. Instead the coefficient $A_{m,n}$ of the $\alpha_{m,n}$ in the optimum linear combination of the $\alpha_{m,n}$ was computed by solving a set of twelve linear equations in the $A_{m,n}$ arising from minimizing $(\alpha_{opt},\alpha_{opt})/L^2(\alpha_{opt}) = \frac{D}{L^2}$ Assuming

$$\alpha_{opt} = \sum_{m=o}^{3} \sum_{n=o}^{2} A_{m,n}\, \alpha_{m,n} \tag{4-24}$$

the $A_{m,n}$ must satisfy the twelve linear equations

$$\frac{\partial \log D/L^2}{\partial A_{p,q}} = 0,\ p=0,\ 1,\ 2,\ 3,\ q=0,\ 1,2$$

or

$$\frac{\partial D}{\partial A_{p,q}} = \frac{2D}{L}\ \frac{\partial L}{\partial A_{p,q}} \tag{4-25}$$

Substituting

$$D = \sum_{m=o}^{3} \sum_{n=o}^{2} \sum_{p=o}^{3} \sum_{q=o}^{2} A_{m,n}\, A_{p,q}\, D_{m,n;p,q} \tag{4-26}$$

$$L = \sum_{m=o}^{3} \sum_{n=o}^{2} A_{p,q}\, L(\alpha_{p,q}) \tag{4-27}$$

$$\frac{\partial D}{\partial A_{p,q}} = 2 \sum_{m=o}^{3} \sum_{n=o}^{2} A_{m,n}\, D_{m,n;p,q}$$

$$\frac{\partial L}{\partial A_{p,q}} = L(\alpha_{p,q})$$

into Eq. 4-25 gives

$$\sum_{m=o}^{3} \sum_{n=o}^{2} A_{m,n} D_{m,n:p,q} = \frac{D}{L} L(\alpha_{p,q}) \tag{4-28}$$

It is easily seen that the $A_{m,n}$ are proportional to D/L whence if we put D=L we are only fixing the scale factor of α_{opt}

Since $D_{m,n;p,q} = D_{p,q;m,n}$ Eq. 4-28 can be written

$$\sum_{p=o}^{3} \sum_{q=o}^{2} A_{p,q} D_{m,n;p,q} = L(\alpha_{m,n}) \tag{4-29}$$

by interchanging the subscripts m,n with p,q. Taking the $D_{m,n;p,q}$ from Table 3 and the $L(\alpha_{m,n})$ from Table 4, the $A_{m,n}$ were calculated by solving Eq. 4-29 on an automatic computing machine. The $A_{m,n}$ were found to be

$$\begin{array}{llll} A_{0,0}= -0.071236 & A_{1,0}= -0.969645 & A_{2,0}= -0.187903 & A_{3,0}= +0.323159 \\ A_{0,1}= +0.445648 & A_{1,1}= -0.664893 & A_{2,1}= -0.608565 & A_{3,1}= -0.094114 \\ A_{0,2}= +0.392242 & A_{1,2}= -0.171329 & A_{2,2}= -0.535262 & A_{3,2}= -0.458589 \end{array} \tag{4-30}$$

The lift, drag, and ℓ/ℓ_f were, by Eq. 4-27

$$L = D = 4.729007K$$

$$\frac{\ell}{\ell_f} = 0.221672 \tag{4-31}$$

The drag reduction obtained by adding α_{opt} for the twelve loadings to the flat plate loading, α_o=1, is given by

$$\frac{\Delta D}{D_f} = \frac{\frac{\ell}{\ell_f}}{1+\frac{\ell}{\ell_f}} = 0.18145 \tag{4-32}$$

or 18.145 percent drag reduction

Among the twelve loadings considered the ones that give the highest drag reduction are, in order, $\alpha_{0,1}$, $\alpha_{0,2}$, $\alpha_{1,0}$ where

$$\alpha_{0,1} = \frac{5}{2}\left(u^3+v^3\right) - \frac{3}{2}(u+v) = \frac{1}{\sqrt{2}}\left[\frac{5}{2}\left(x^3+3xy\right) - 3x\right]$$

$$\alpha_{0,2} = \frac{1}{8}\left[63\left(u^5+v^5\right) - 70\left(u^3+v^3\right) + 15(u+v)\right]$$

$$= \frac{x}{16\sqrt{2}}\left[63\left(x^4+10x^2y^2+5y^4\right) - 140\left(x^3+3y^2\right) + 60\right]$$

$$\alpha_{1,0} = \frac{3uv}{2}(u+v) - \frac{1}{2}(u+v) = \frac{1}{\sqrt{2}}\left[\frac{3}{2}x(x^2-y^2) - x\right]$$

On the other hand $\alpha_{0,0} = u + v = 2x/2$ contributes very little to the drag reduction. From this one is led to the conclusion that the major drag reduction among the first six loadings is actually due to using the α-distributions which vary with x^3 and with xy^2 in an optimal combination. The further drag reduction effected by the remaining loadings is probably primarily due to the loading x^3y^2 or xy^4.

Fig. 4-2 and 4-3 are graphs which show the angle of attack distribution for the diamond planform with optimal loading, and the pressure distribution corresponding to this α-distribution. The latter was calculated on an automatic computing machine. From the requirements for an optimum planform, Eqs. 3-12 and 3-13, it can be shown that the optimum pressure distribution will be symmetric about the y axis when the planform is symmetric about this axis. The lack of symmetry evidenced in Fig. 4-3 is caused by approximating the α distribution by only a finite number of Legendre polynomials. It should be pointed out that the flat plate pressure distribution is far from symmetric so that the distribution of Fig. 4-3 qualitatively does approach the desired optimum quite closely

α_B DISTRIBUTION FOR DIAMOND PLANFORM

$$\alpha_{OPT} \approx \alpha_0 (1 + \alpha_B)$$

$$\alpha_0 = D_{OPT} / L_{OPT}$$

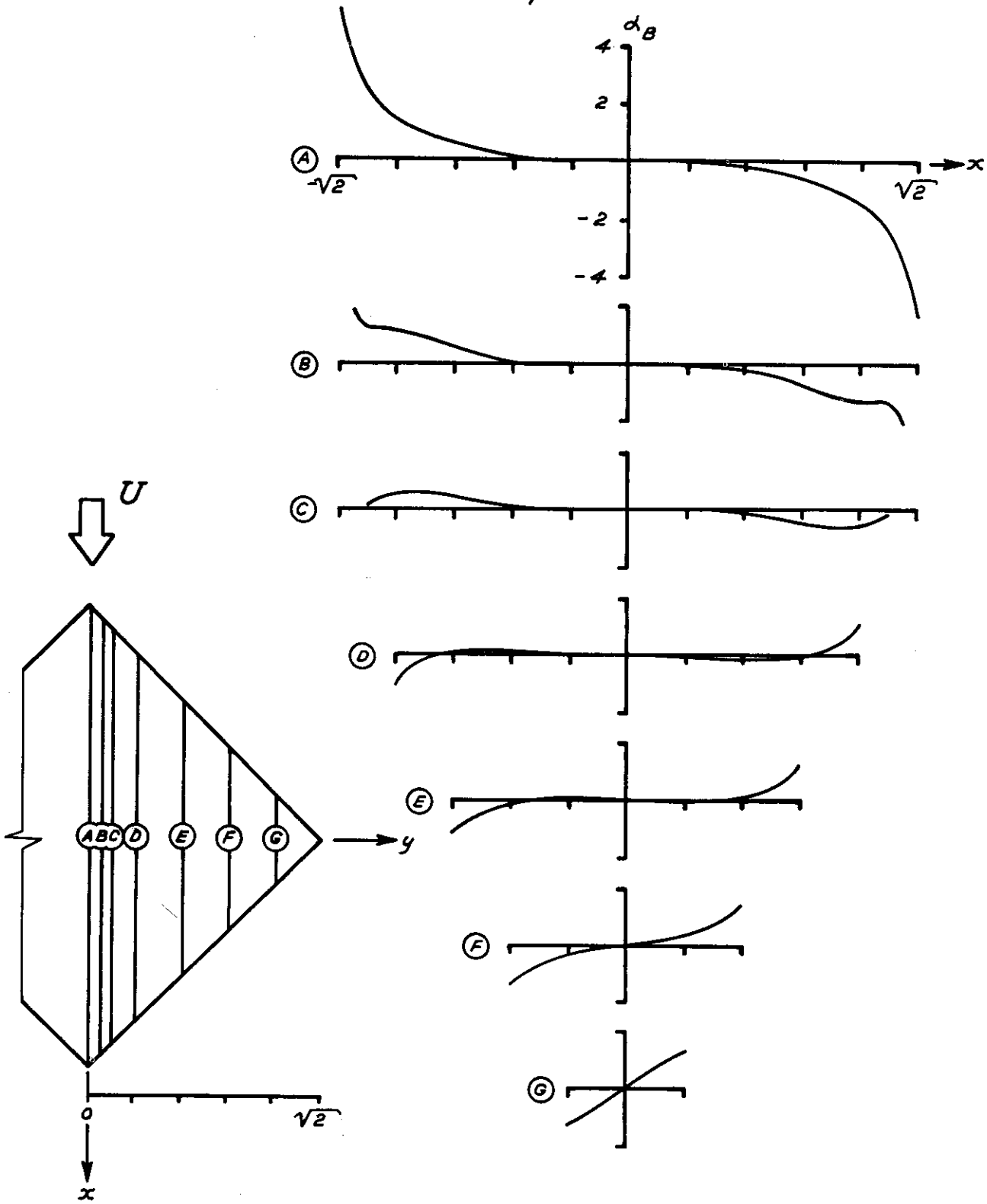

FIGURE 4-2

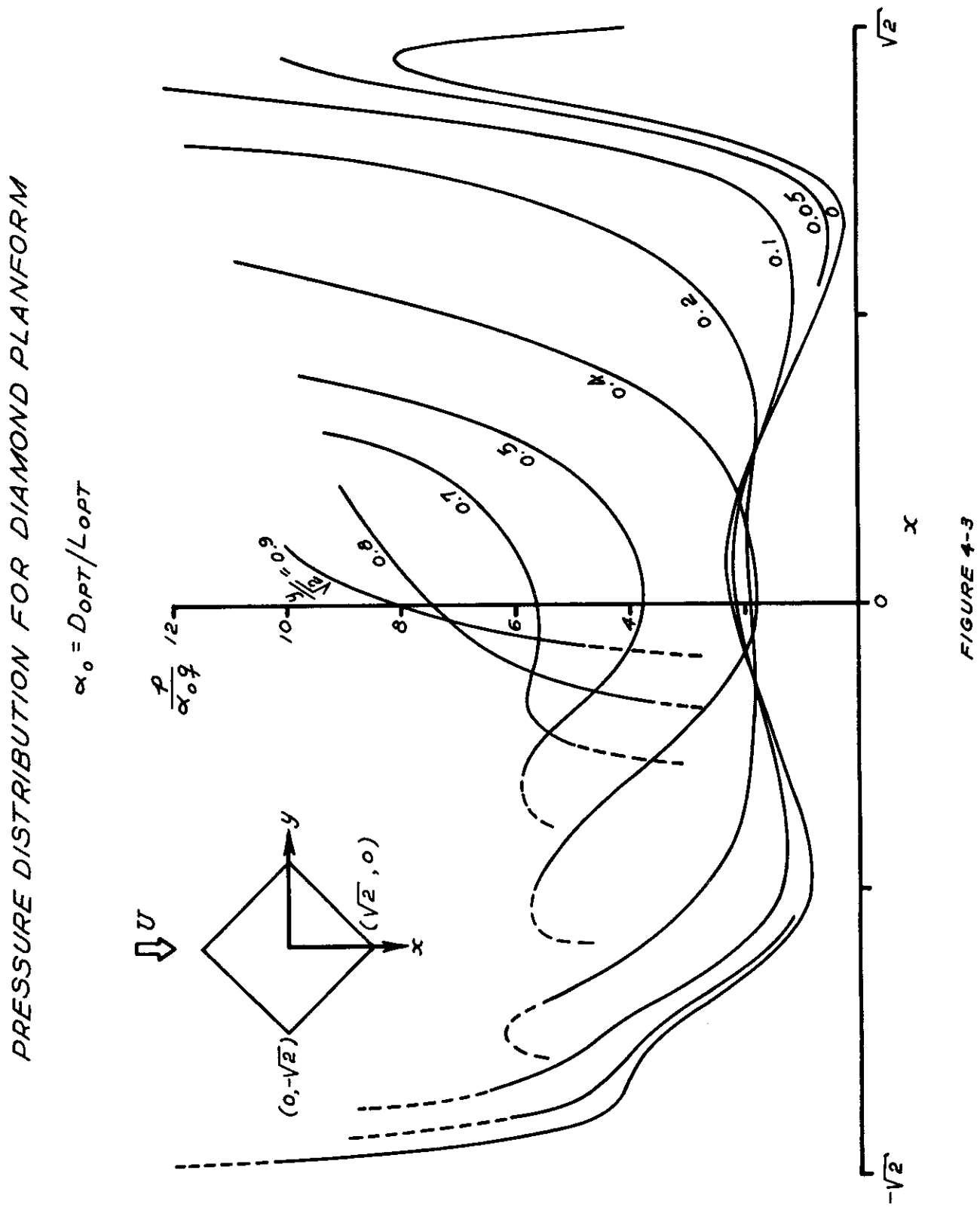

FIGURE 4-3

over a large portion of the wing. One of the conditions for minimum drag neglected in the approximation for α is that the leading edge meet the free stream at zero angle of attack so that the pressure will be finite. The α distribution of Fig. 4-2 has leading edge values greater than zero near the center and less than zero near the tips; consequently the pressure becomes infinite at the leading edge.

5. SOME LOW-DRAG GEOMETRIES FOR THE RECTANGULAR WING

In this section the optimal loading for the rectangular planform will be determined for several restricted classes of loadings. The notation illustrated by Fig. 5.1 will be used.

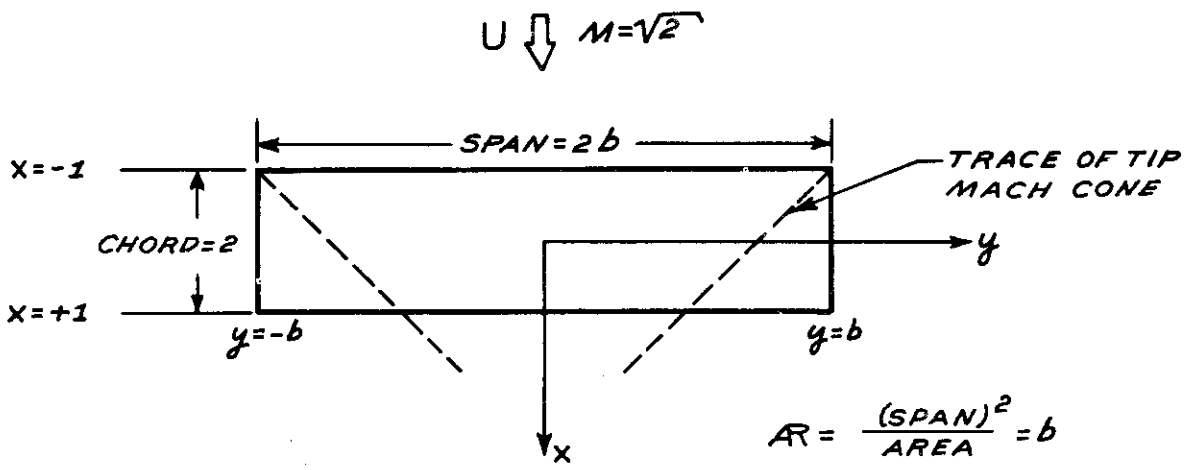

Fig. 5.1 Notation for Rectangular Wing

In general, the results will be valid only for $AR \geq 1$, although in some special cases the applicability of the formulas will be restricted to even higher aspect ratios.

To begin with, a class of loadings C_1 and its subclass C_2 will be discussed where

C_1: Loadings with α independent of y (5-1a)

C_2: Loadings in C_1 with α odd in x (5-1b)

According to Eq. 3-12 and 3-13 the optimal loading in C has an angle of attack distribution which is the sum of a constant and the optimal angle of attack in C_2. This optimum has been found by Rott[8] and independently by R. Sedney[10]. Sedney's derivation is based on the integral equation, Eq. 3-18, or rather on its analogue for the restricted class C_2. This derivation will now be described. Consider a strip extending across the wing

parallel to the y-axis located between $x = \xi$ and $x = \xi + \Delta\xi$. Let the angle of attack be α on this strip, zero elsewhere and let $\alpha\Delta\xi = 1$. The limiting case as $\Delta\xi \to 0$ will be referred to as a unit strip at x. In this case the angle of attack distribution is $\delta(x - \xi)$. We then define

$$\ell(\xi;x) = \text{chordwise lift at x due to a unit strip at } \xi \tag{5-2}$$

This function is the equivalent, for C_2, of the Green's function defined for the general case by Eq. 3-15a. From the formulas for the rectangular wing it follows immediately that for $AR \geq 1$

$$\ell(\xi;x) = \ell(x-\xi) = \begin{cases} 4q\left[2b\,\delta(x-\xi) - 1\right] & \text{IF } x \geq \xi \\ 0 & \text{IF } x < \xi \end{cases} \tag{5-3}$$

For an arbitrary loading in C_2, $\alpha = f(x)$, the total lift and drag are then

$$L(f) = \int_{-1}^{+1}\int_{-1}^{+1} \ell(x-\xi) f(\xi)\, d\xi dx \tag{5-4a}$$

$$D(f) = \int_{-1}^{+1}\int_{-1}^{+1} \ell(x-\xi) f(x) f(\xi)\, d\xi dx \tag{5-4b}$$

In particular the total lift due to a unit strip at ξ is

$$L\left[\delta(x-\xi)\right] = \int_{-1}^{+1} \ell(x-\xi)dx = 4q\left[2b - (1-\xi)\right] \tag{5-5}$$

The optimum loading within the restricted class C_2 must satisfy the relation

$$D(f) + \lambda L(f) = \text{MINIMUM} \tag{5-6}$$

where λ is a Lagrangian multiplier whose value will be determined below.

This equation implies

$$\lim_{\varepsilon \to 0} \frac{\left[D(f+\varepsilon g) + \lambda L(f+\varepsilon g)\right] - \left[D(f) + \lambda L(f)\right]}{\varepsilon} = 0 \qquad (5\text{-}7)$$

for an arbitrary function g(x). Eq. 5-7 is equivalent to

$$\int_{-1}^{+1} \left[\ell(\xi - x) + \ell(x - \xi)\right] f(\xi)\, d\xi + \lambda \int_{-1}^{+1} \ell(\xi - x)\, d\xi = 0 \qquad (5\text{-}8)$$

By multiplying this equation by f(x) and integrating over x one finds that

$$\lambda = \frac{-2D}{L} \qquad (5\text{-}9)$$

The integral equation, Eq. 5-8, is the equivalent for C_2 of the general equation, Eq. 3-16. This relation can be derived from Eq. 3-14 if α_{opt} in that equation is taken to be the optimal loading in C_1 and α the special loading $\delta(x - \xi)$ (cf. a similar derivation below for the class C_5). Inserting the value of $\ell(x-\xi)$ into Eq. 5-8, one obtains

$$-\int_{-1}^{+1} f(\xi)\, d\xi + 4b f(x) + \lambda \left[-(1-x) + 2b\right] = 0 \qquad (5\text{-}10)$$

As mentioned earlier the optimal loading $\alpha = f(x)$ may be written

$$\alpha_{OPT\ IN\ C_1} = f(x) = \alpha_0 \left[1 + g(x)\right] \qquad (5\text{-}11)$$

when α_0 is a constant and g(x) is an odd function. The integral term in Eq. 5-11 is then simply $-2\alpha_0$ and the equation reduces to the algebraic relation

$$\left[(2b-1)(\lambda + 2\alpha_0)\right] + \left[4b\alpha_0 g(x) + \lambda x\right] = 0$$

Since the first term is a constant and since the equation must be true for any value of x it follows that

$$\lambda = -2\alpha_o \quad , \qquad g(x) = \frac{-\lambda x}{4b\alpha_o} = \frac{x}{2b} = \frac{x}{2AR} \tag{5-12}$$

Hence the loadings of the type

$$\alpha_1 = \alpha_o\left(1 + \frac{x}{2AR}\right) \quad , \qquad \alpha_o = CONSTANT \tag{5-13}$$

are optimal within the class C_1 of loadings which are independent of y. This result is valid for rectangular wings of $AR \geq 1$.

Thus within the class C_2 of α's which are odd in x and independent of y the parabolic arc shape (or any multiple thereof)

$$\alpha_2 = x \tag{5-14}$$

is the optimum. Let L_1 and D_1 be the lift and drag of α_1 as defined by Eq. 5-13 and L_2 and D_2 the lift and drag of α_2. It then follows from Eq. 3-11a that

$$\frac{D_1 L_2}{L_1 D_2} = \frac{\alpha_o}{2AR} \quad OR, \; SINCE \; \alpha_o = -\frac{\lambda}{2} = \frac{D_1}{L_1} \; BY \; Eq. \; 5\text{-}9$$

$$\frac{L_2}{D_2} = \frac{1}{2AR} \tag{5-15a}$$

From Eq. 5-3 and 5-4, or from Eq. 5-5, it follows that

$$L_2 = \frac{8q}{3} \tag{5-15b}$$

The optimal ℓ in C_2 is

$$\ell_{2OPT} = \frac{L_2^2}{D_2 qS} = \frac{1}{3AR^2} \tag{5-15c}$$

Now for the loading on a rectangular flat plate

$$\ell_f = \frac{dC_L}{d\alpha} = 4\left(1 - \frac{1}{2AR}\right) \tag{5-16}$$

so that from Eq. 3-11c and 5-15a the optimal ℓ in C_1 is then

$$\ell_{1OPT} = \frac{L_1^2}{D_1 qS} = \ell_f + \ell_{2OPT} = 4\left(1 - \frac{1}{2AR} + \frac{1}{12AR^2}\right) \qquad (5\text{-}17)$$

for AR $\geq$ 1.

For rectangular wings with AR > 2 it is useful to consider certain regions according to their spanwise location: part of the outer or tip regions, $b - 2 \leq |y| \leq b$, is affected by the side edges; no part of the inner or middle region, $|y| \leq b - 2$ (which exists only when AR > 2), is affected by the side edges. Since the camber is symmetric, α is odd in x. Hence, the integral of α over the middle section is zero. It then follows from Theorem I of Ref. 9 that the lift contributed by the camber in the middle section is zero. On the other hand, the drag there is not zero. It is plausible, then, that the drag due to lift may be decreased by a spanwise variation in camber - in particular by a decrease in camber in the middle section. We shall first study a simplified case of such variation. For convenience we define two functions of y:

$$T(y) = \begin{cases} 0 \text{ in the middle section} \\ 1 \text{ in the tip section} \end{cases} \qquad (5\text{-}18a)$$

$$M(y) = \begin{cases} 1 \text{ in the middle section} \\ 0 \text{ in the tip section} \end{cases} \qquad (5\text{-}18b)$$

and we consider the two restricted classes of loadings

C_3: Loadings of the form $\alpha = g(x)M(y) + f(x)T(y)$ (5-19a)

C_4: Loadings in C_3 with α odd in x (5-19b)

Thus $\alpha = f(x)$ in the tip regions and $\alpha = g(x)$ in the middle section.

The optimum in C_4 will first be found for AR $\geq$ 3. Some auxiliary formulas can now be introduced. Consider a unit strip located at $x = \xi_1$, and

extending only between y = -(b-2) and y = (b-2), that is, the middle section (see Fig. 5.2). The angle of attack distribution is then $\alpha(x,y) = M(y)\,\delta(x - \xi_1)$. The pressure downstream of the strip is zero except in the Mach cones from E and F. The total lift on a strip extending from A_1 to A_2 at a chordwise station $\xi_2 > \xi_1$ is zero (cf Ref. 9, Theorem I).

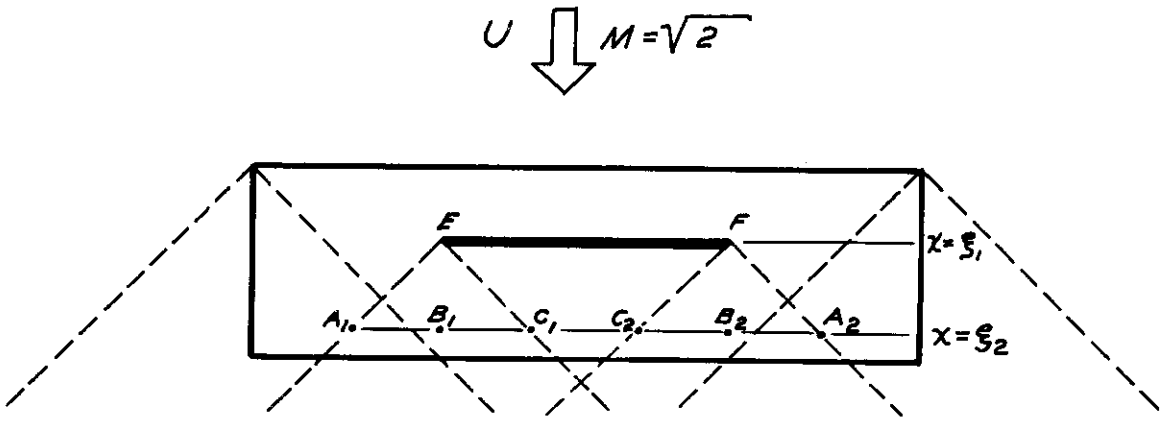

Fig. 5.2 Unit Strip in Middle Section, AR ≧ 3

Let the lift between A_1 and B_1 at $x = \xi_2$ due to the corner effect at E be $4q\sigma$. It then follows from symmetry arguments that the lift carried between B_1 and C_1 is $-4q\sigma$. (Note that if the Mach cones from E and F overlap at $x = \xi_2$ this statement is true only for the effect of E alone.) From the fact that the pressure distribution may be obtained as an x-derivative of a conical pressure distribution (cf. the distribution of Eq. 5-42 below), it follows that σ is independent of ξ_2 as long as $\xi_2 \geq \xi_1$. Actually

$$\sigma = \frac{1}{\pi} \tag{5-20}$$

although for the following only the fact that σ is a constant will matter.

Consider now the two elementary loadings from the class C_4

$$\alpha^*(x,y) = \tau(y)\,[\delta(x-\xi_1) - \delta(x+\xi_1)] \tag{5-21a}$$

$$\alpha^{**}(x,y) = M(y)\left[\delta(x-\xi_2) - \delta(x+\xi_2)\right] \qquad (5\text{-}21b)$$

These loadings are shown in the figure below:

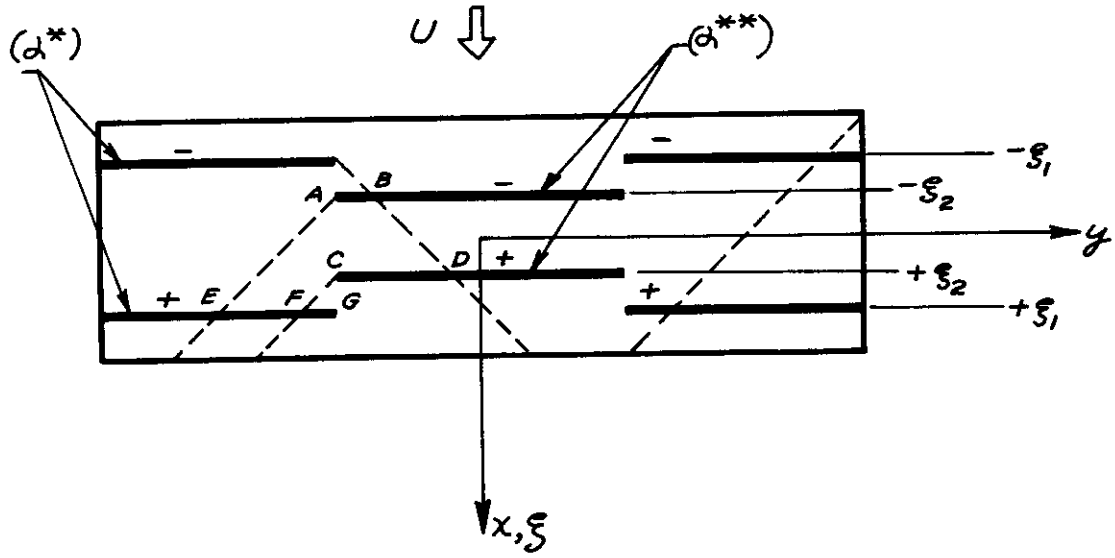

Because of symmetry, the interference drag (α^*, α^{**}) is twice that obtained by considering only half the wing. If we define p_1, p_2, and p_3 as the pressure distributions due to $T(y)\,\delta(x+\xi_1)$, $M(y)\,\delta(x+\xi_2)$ and $M(y)\,\delta(x-\xi_2)$, respectively, then

$$(\alpha^*,\alpha^{**}) = 2 \lim_{dx\to 0}\left\{ -\int_A^B \int_{-\xi_2-\frac{dx}{2}}^{-\xi_2+\frac{dx}{2}} p_1\,\alpha^{**}\,dx\,dy \;-\; \int_C^D \int_{\xi_2-\frac{dx}{2}}^{\xi_2+\frac{dx}{2}} p_1\,\alpha^{**}\,dx\,dy \right.$$
$$\left. -\int_E^G \int_{\xi_1-\frac{dx}{2}}^{\xi_1+\frac{dx}{2}} p_2\,\alpha^{*}\,dx\,dy \;+\; \int_F^G \int_{\xi_1-\frac{dx}{2}}^{\xi_1+\frac{dx}{2}} p_3\,\alpha^{*}\,dx\,dy \right\}$$

Then, since by definition

$$\lim_{dx\to 0} \int \alpha\,dx = 1\cdot(\text{SIGN OF } \alpha),$$

$$(\alpha^*,\alpha^{**}) = 2\left[\int_A^B p_1\,dy - \int_C^D p_1\,dy - \int_E^G p_2\,dy + \int_F^G p_3\,dy\right]$$

for $\xi_1 \geq \xi_2$ as shown in the figure. Because of the constancy of σ, each of these integrals is equal to $4q\sigma$ and the interference drag thus is zero; a similar argument holds for $\xi_2 > \xi_1$ so that

$$\left(\alpha^*, \alpha^{**}\right) = 0 \tag{5-22}$$

for $AR \geq 3$. Consider further two loadings of C_4 of the form

$$\alpha' = T(y)\, f(x) \tag{5-23a}$$

$$\alpha'' = M(y)\, g(x) \tag{5-23b}$$

where f and g are odd functions. Since f and g may be approximated by series of the form $\sum a_i \left[\delta(x-\xi_i) - \delta(x+\xi_i)\right]$, $0 \leq \xi_i \leq 1$

it follows from Eq. 5-22, by superposition, that

$$\left(\alpha', \alpha''\right) = 0 \tag{5-24}$$

for $AR \geq 3$.

Now any loading in C_4 (Eq. 5-19b) may be written in the form $\alpha' + \alpha''$ where α' and α'' are defined as in Eq. 5-23. The loading α'' has zero lift whereas its drag is greater than zero except for $g(x) = 0$. This fact together with the orthogonality relation (Eq. 5-24) implies that for any fixed choice of $f(x)$ the optimal choice of $g(x)$ is zero. Thus, for $AR \geq 3$[//] the optimal loading in C_3 and C_4 are the same as the optimal loadings in the sub-classes

//Note that for $AR \geq 3$ the aspect ratio of the middle section is ≥ 1. It is known that a rectangular wing at zero angle of attack with thickness distribution which is even in x and independent of y has a drag coefficient which is independent of aspect ratio for $AR \geq 1$. This fact is closely related to Eq. 5-24 and may be proved by the same symmetry principles. A simple case of this drag formula was found in Ref. 11 and was explained in terms of conical symmetry by R. T. Jones.

C_5 and C_6, respectively, where

C_5: Loadings of the form $\alpha = f(x)\ T(y)$ (5-25a)

C_6: Loadings in C_5 with α odd in x (5-25b)

The optimum in C_6 may be found in the same manner as the optimum in C_1. To illustrate the fact that several methods are available, the integral equation corresponding to Eq. 5-11 will be derived by a variant of the method previously used. We start with the general equation where we let $\alpha_{opt} = f(x)\ T(y)$ be the optimum in C_6 and $\alpha = \alpha^*$ as defined by Eq. 5-21a. Since $\alpha^* = \delta(x - \xi) - \delta(x + \xi) - \alpha^{**}$ and $L(\alpha^{**}) = 0$ it follows from Eq.5-5 that

$$L(\alpha^*) = 8q\xi \tag{5-26}$$

If p^* is the pressure distribution corresponding to α^* we define

$$P(x) = \int p^*(x,y)\,dy \qquad \text{FOR } b-2 \le |y| \le b \tag{5-27a}$$

and

$$P_o(x) = \text{ODD PART OF } P(x) = \frac{P(x) - P(-x)}{2} \tag{5-27b}$$

Then

$$\int \alpha_{OPT}\, p^*\, dS = \int_{-1}^{+1} f(x) P(x) dx = 2\int_0^1 f(x)\, P_o(x) dx \tag{5-28}$$

To evaluate P(x), note that the pressure in the tip regions caused by the outer tip of the loading $T(y)\ \delta(x - \xi)$ is the same as that caused by $\delta(x - \xi)$. Thus, for $x > \xi$ we may use the result for $\ell(\xi; x)$ given in Eq. 5.3, adding to it the contribution from the inner edges, $|y| = b - 2$ (cf. the discussion preceeding Eq. 5-20). Thus, for the loading $T(y)\ \delta(x - \xi)$

$$\ell(\xi; x) = 4q\left[4\delta(x-\xi) - 1 - 2\sigma\right], \qquad x \ge \xi$$

With the corresponding result for $\ell\,(-\xi\,;x)$, P(x) may be determined, and from Eq. 5-27b,

$$P_o(x) = 8q\left[\delta(x-\xi) - \delta(x+\xi)\right] \quad , \qquad 0 \le x \le 1 \tag{5-29}$$

If one now lets α_{opt} in Eq. 5-14 be the optimum in C_6 and α the α^* defined by Eq. 5-21a one obtains with the aid of Eq. 3-9, 5-26, 5-28, and 5-29:

$$4f(\xi) = \frac{D_{OPT}}{L_{OPT}}\,\xi \tag{5-30}$$

Thus, the integral equation, Eq. 3-14, for f(x) immediately reduces to the trivial equation, Eq. 5-30. This is due to the fact that the kernal $P_o(x)$ consists of delta functions only. According to Eq. 5-30, α_6 or any multiple thereof is an optimum in C_6 where

$$\alpha_6 = xT(y) \tag{5-31}$$

If L_6 and D_6 are the lift and drag of α_6 then by Eq. 5-30

$$\frac{D_6}{L_6} = 4 \tag{5-32a}$$

Furthermore, $\alpha_6 = xT(y)$ has the same lift as $\alpha_2 = x$ so that according to Eq. 5-15b

$$L_6 = \frac{8q}{3} \tag{5-32b}$$

The optimum ℓ in the class C_6 is then

$$\ell_{6\,OPT} = \frac{1}{6AR} \tag{5-33}$$

Combining α_6 with a flat plate loading we obtain that the optimum C_5 is of the form

$$\alpha_5 = \alpha_o\left[1 + \frac{xT(y)}{4}\right] \quad , \quad \alpha_o = CONST. = \frac{D_5}{L_5} \tag{5-34}$$

The optimum ℓ in C_5 is then

$$\ell_{5_{OPT}} = \ell_f + \ell_{6_{OPT}} = 4\left(1 - \frac{1}{2AR} + \frac{1}{24AR}\right) \tag{5-35}$$

This formula is valid for the class C_5 for $AR \geq 3$. The class C_5, in which the spanwise variation of camber is stepwise, contains the class C_1, where camber is constant spanwise. A comparison of Eq. 5-33 and Eq. 5-17 shows the improvement obtained by allowing the camber to vary.

For $AR < 3$ the tip sections overlap and the middle section has $AR < 1$ so that the drag coefficient of xM(y) is no longer two-dimensional. These facts invalidate the derivation of Eq. 5-33. A related formula valid for $2 \leq AR < 3$ will now be discussed. Consider the class of distributions

$$C_7: \quad \alpha = Ax\,T(y) + Bx\,M(y) \tag{5-36}$$

where A and B are arbitrary constants.

To find the optimum for this class, consider the two loadings

$$\alpha' = x \tag{5-37a}$$

$$\alpha'' = x\,M(y) \tag{5-37b}$$

If L' and D' are the lift and drag of α', and L" and D" those of α'', it then follows from Eq. 5-15a and 5-15b that

$$L' = \frac{8q}{3} \tag{5-38a}$$

$$D' = \frac{16qAR}{3} \tag{5-38b}$$

As stated previously

$$L'' = 0 \tag{5-39}$$

D" cannot easily be evaluated by elementary superposition procedures because the aspect ratio of the middle section is less than unity. To determine D", first consider a unit strip of width 2(b-2) at ξ as shown in

Fig. 5.3. If this strip is at an angle

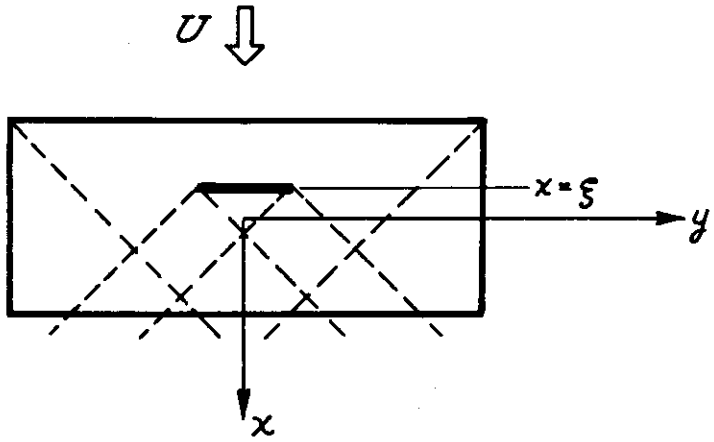

Fig. 5.3

Unit Strip in Middle Section, $2 < AR \leq 3$

of attack α the pressure distribution induced on the wing can be determined from the solution for a deflected control surface. The latter solution in the region (ABC) of Fig. 5.4 is (Ref. 11)

$$p = \frac{4q\alpha}{\pi} \cos^{-1}\left(\frac{y}{x}\right) \quad , \qquad \left|\frac{y}{x}\right| \leq 1 \tag{5-40}$$

where the control surface is at an angle of attack α and the rest of the wing is at $\alpha = 0$; p is the pressure difference between lower and

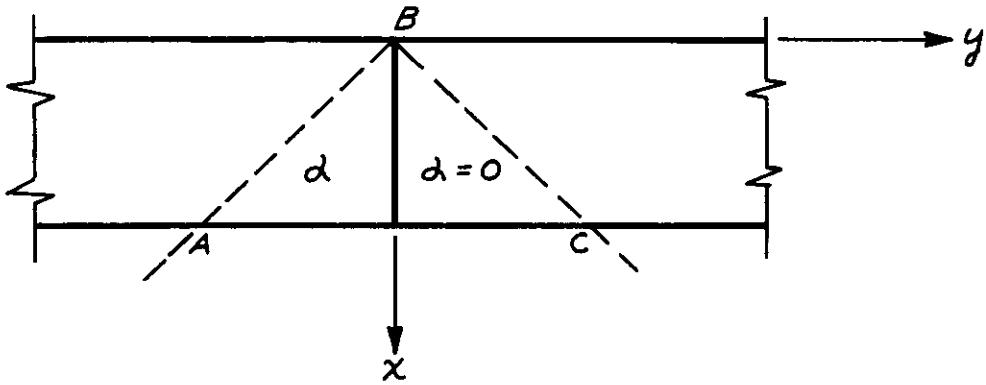

Fig. 5.4

Wing and Control Surface Junction

upper surfaces. The pressure distribution due to a semi-infinite unit strip can be derived by differentiation of Eq. 5-40 with $\alpha = 1$. By subtracting a similar solution shifted the width of the middle section the pressure distribution caused by the finite span unit strip in Fig. 5.3 is obtained. In the tip Mach cones, the corner effects are

$$\Delta p = \frac{4q}{\pi}\left[\frac{y-(b-2)}{\sqrt{(x-\xi)^2-(y-b+2)^2}} - \frac{y+b-2}{\sqrt{(x-\xi)^2-(y+b-2)^2}}\right], \quad \left|\frac{|y|-(b-2)}{x-\xi}\right| \le 1 \qquad (5\text{-}41)$$

At the strip itself Δp has the two-dimensional value $4q$. The formula for $\ell(\xi;x)$ as defined in Eq. 5-2, for the middle section only, is

$$\ell(\xi;x) = \int_{-(b-2)}^{b-2} \Delta p\, dy + 8q(b-2)\delta(x-\xi) \qquad (5\text{-}42)$$

D" is then determined from Eq. 5-4b, 5-41, and 5-42;

$$D'' = \frac{16q(AR-2)}{3F(AR)}, \qquad 2 \le AR \le 3 \qquad (5.43)$$

where

$$F(AR) = \frac{1}{1+\frac{3\lambda}{\pi}\left(1-\frac{\lambda^2}{6}\right)\cosh^{-1}\frac{1}{\lambda} - \frac{\lambda}{2\pi}\sqrt{1-\lambda^2} - \frac{2}{\pi}\cos^{-1}\lambda}$$

and $\lambda = AR - 2$ is the aspect ratio of the middle section.

In determining the interference drag (α', α'') of the two α distributions (Eq. 5-37), we next examine the effect of a unit strip of one distribution on a unit strip of the other. There are three cases to consider, as shown in Fig. 5.5.

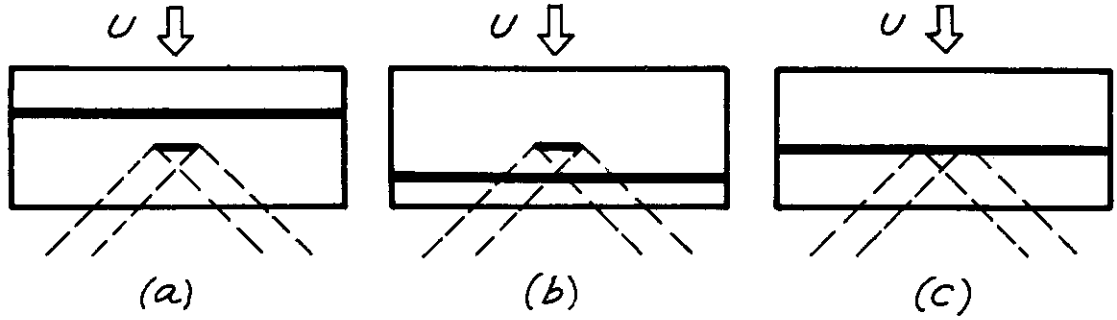

Fig. 5.5

Cases Involved in Determination of (α', α'')

In the first case, the longer strip is ahead of the shorter so there is no interference drag due to the pressure distribution of the shorter; also since the shorter is in the two-dimensional region behind the longer there will be no pressures induced on the shorter. Thus, there is no interference drag in this case. If the longer strip is behind the shorter as in Fig. 5-5b, it will not induce pressures on the latter, and also, by application of Theorem I in Ref. 9, the total lift induced by the shorter on the longer will be zero. Thus, again there is no interference drag. The only interference drag which exists occurs when one strip is superimposed on the other; in this case the drag is two-dimensional and is

$$(\alpha', \alpha'') = 2[2(b-2)]\int_{-1}^{1} 4q\alpha'\alpha'' dx = \frac{32q(AR-2)}{3} \qquad (5\text{-}44)$$

since b = AR .

The optimal α in C_7 may be written in the form

$$\alpha_7 = A'x + B'x\,M(y) \qquad (5\text{-}36')$$

where A' and B' have to be determined. Let L_7 and D_7 be the lift and drag of α_7. From Eq. 5-38 and 5-39

$$L_7 = \frac{8qA'}{3} \qquad (5\text{-}45)$$

and from Eq. 5-38, 5-43, and 5-44,

$$\begin{aligned} D_7 &= A'^2 D' + B'^2 D'' + A'B'(\alpha', \alpha'') \\ &= \frac{16q}{3}\left[A'^2 AR + \frac{(AR-2)B'^2}{F(AR)} + 2(AR-2)A'B'\right] \end{aligned} \qquad (5\text{-}46)$$

Since L_7 is independent of B', D_7 can be minimized with respect to B' by setting $\partial D_7/\partial B' = 0$. This gives

$$B = -A'F(AR)$$

Hence, the optimum in C_7 if of the form

$$\alpha_7 = A'x\left[1 - F(AR)M(y)\right] , \qquad A' = \text{CONSTANT} \qquad (5\text{-}47a)$$

and

$$D_7 = \frac{16qA'^2}{3}\left[AR - (AR-2)F(AR)\right] \tag{5-47b}$$

The optimum ℓ in the class C_7 is then

$$\ell_{7OPT} = \frac{1}{3AR\left[AR-(AR-2)F(AR)\right]} \tag{5-48}$$

The optimum in the class C_8 formed by superposition of flat plate loadings and loadings from C_7 is then

$$\alpha_8 = \alpha_0\left\{1 + \frac{\chi\left[1-F(AR)M(y)\right]}{2\left[AR-(AR-2)F(AR)\right]}\right\} \tag{5-49}$$

where α_0 = constant = $\frac{D_8}{L_8}$; the corresponding ℓ is

$$\ell_{8OPT} = \ell_f + \ell_{7OPT} = 4\left\{1 - \frac{1}{2AR} + \frac{1}{12AR\left[AR-(AR-2)F(AR)\right]}\right\} \tag{5-50}$$

For AR = 3, F(AR) = 1 and Eq. (5-50) reduces to the result given by Eq. 5-35. For $2 < AR < 3$, $F(AR) > 1$ and there must be negative camber in the center section if the lift is positive.

As a last problem we shall study the introduction of further spanwise variation. Consider a wing of AR > 3 with an α distribution as shown in Figure 5.6.

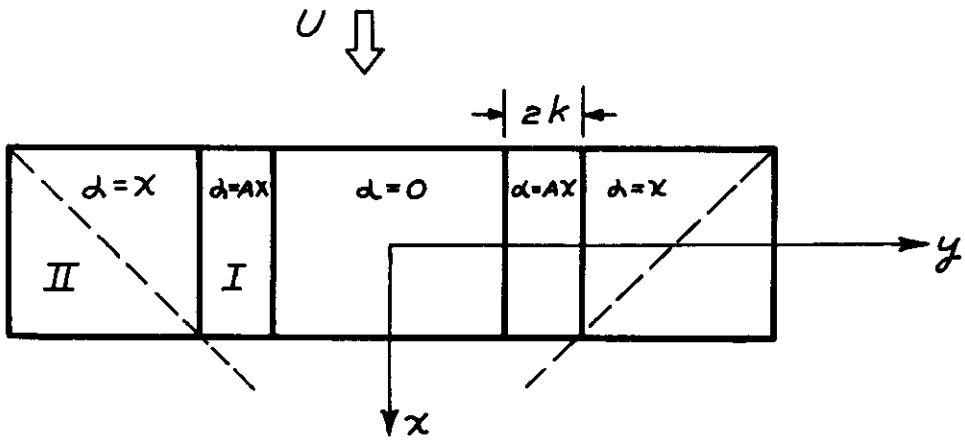

Fig. 5.6

Special Spanwise Variation of α

The values of A and k which give maximal ℓ will be found under the assumption that the section where $\alpha = 0$ has $AR \geq 1$, i.e., $(b - 2 - 2k) \geq 1$.

The left half of the wing does not interfere with the right half. Hence, to compute the drag it is sufficient to find the drags of Sections I and II and their interference drag. The drag of II, D_{II}, has been computed previously. The drag of I, D_I, is a quadratic function of A and is hence

$$D_I(A) = A^2 D_I(1)$$

where $D_I(1)$ is given by Eq. 5-43 with k replacing the quantity (AR - 2).

The interference drag $D_{I\ II}$ is a linear function of A and hence

$$D_{I\,II}(A) = A D_{I\,II}(1)$$

Here $D_{I\ II}(1)$ is easily determined from previous results since the interference drag is unchanged if a plate with $\alpha = 0$ is placed adjacent to the outboard tip. Denote the corresponding drags when $\alpha = 0$ to the right of the wing by primes; then $D'_I = D_I$, $D'_{I\ II} = D_{I\ II}$ and hence, if D'_{I+II} is the total drag,

$$D'_{I+II} = D_I + D'_{II} + D_{I\,II}$$

In this equation all terms are known except the last which is thus determined. We may then write the drag of the wing in Fig. 5.6 as

$$D = \frac{32q}{3}\left\{1 + \frac{A^2 k}{F(k)} + kA\left[1 - \frac{1}{F(k)}\right]\right\} \qquad (5\text{-}51)$$

The lift is $L = 8q/3$ since the distribution $\alpha = Ax$ carries zero total lift. Minimizing Eq. 5-51 in the usual manner places the following restrictions on A and k:

$$A = -\frac{1}{2}\left[F(k) - 1\right]$$

and

$$\frac{\partial F}{\partial k} = \frac{-F(F-1)}{k(F+1)} \tag{5-52}$$

The value of k for minimum drag, as determined graphically, is

$$k \cong 0.025$$

Then

$$A \cong -3.20$$

$$D \cong \frac{(0.958)32q}{3} \tag{5-53}$$

and

$$\ell \cong \frac{1.043}{6AR}$$

For convenience, define

$$B(y) = \begin{cases} 1 & b-2k-2 \le |y| \le b-2k \\ 0 & \text{ELSEWHERE} \end{cases}$$

Combining the α distribution leading to Eq. 5-53 with the flat plate results in the final optimum,

$$\alpha_{g_{OPT}} \simeq \alpha_o \left[1 + 0.261 \times T(y) - 0.834 \times B(y)\right] \tag{5-54a}$$

and

$$\ell_{g_{OPT}} \simeq 4\left[1 - \frac{1}{2AR} + \frac{1.043}{24AR}\right], \qquad AR \geq 3.05 \tag{5-54b}$$

This is a slight improvement over the optimum obtained in Eq. 5-35 for the simpler α distribution.

We shall now discuss certain general qualitative properties of the absolute optimum for the rectangular wing. This optimum has the form $\alpha_{opt} = \alpha_A + \alpha_B$, $p_{opt} = p_A + p_B$ where α_A = constant and α_B is odd in x. Furthermore, p_{opt} is even in x since the class of loadings is not restricted. In the middle section p_A is constant and hence, in particular, even in x.

It then follows that p_B is even in x in the middle section. Since α_B is odd, the drag per unit span of the loading α_B must be zero in the middle section:

$$\int_{-1}^{+1} p_B \alpha_B \, dx = 0, \qquad |y| \leq b-2 \tag{5-55}$$

One may easily generalize Eq. 5-55 as follows. In Eq. 3-14, let α_{opt} be the optimum in the restricted class of loadings which are odd in x, i.e., α_B; let α be $\delta(y - y_o)\, \alpha_B(x,y)$ and $L(y_o)$ denote the lift of α. Then, since

$$(\alpha_B, \alpha) = 2 \iint_S \delta(y-y_o) \alpha_B(x,y) p_B(x,y) \, dx\, dy$$

$$= 2 \int_{-1}^{+1} \alpha_B(x,y_o) p_B(x,y_o) \, dx$$

Eq. 3-14 reduces to

$$\int_{-1}^{+1} \alpha_B(x,y_o) p_B(x,y_o) \, dx = \frac{D_B \, L(y_o)}{L_B} \tag{5-56}$$

In words, this equation states that the drag per unit span, at the spanwise station y_o, of the optimal loading α_B is $\frac{D_B}{L_B}$ times the lift caused by the strip, $\delta(y-y_o)\alpha_B(x,y)$, at the same station. In the middle section this lift is zero by the previously quoted Theorem I of Ref. 9. Thus Eq. 5-55 is seen to be a special case of Eq. 5-56.

Eq. 5-55 is, of course, satisfied for loadings when $\alpha = 0$ in the middle section. However, it is easy to construct nontrivial loadings which also have the same property. The following idea may be used to construct solutions of Eq. 5-55. To fix the ideas, consider only α's of the form $xf(y)$ where $f(y)$ is even in y. Since we are concerned with the middle section

only, we may, to begin with, consider the wing to be of infinite aspect ratio. The station y = 0 then plays no distinguished role. It is natural to expect that if f(y) is a solution, and if one takes as a new solution that part of f(y) which is even around any station $y = y_o$, then this new solution is a multiple of the original solution, the coefficient depending on y_o.

Putting $Z = y - y_o$ one then obtains the functional equation

$$f(y_o+Z) + f(y_o-Z) = 2g(y_o)f(Z) \tag{5-57a}$$

Putting Z = 0 gives

$$g(y_o) = \frac{f(y_o)}{f(0)} \tag{5-57b}$$

where one may normalize

$$f(0) = 1 \tag{5-57c}$$

so that Eq. 5-57 may be written

$$f(y_o+Z) + f(y_o-Z) = 2f(y_o)f(Z) \tag{5-58}$$

with f(y) even, f(0) = 1. Solutions of Eq. 5-58 are

$$f(y) = \cos ay \tag{5-59a}$$

or

$$f(y) = \cosh by \tag{5-59b}$$

where a and b are constants which must be determined by substituting $\alpha = xf(y)$ into the integral equation, Eq. 5-55. It is found that only the hyperbolic cosine term satisfies the integral equation, and then

only for one value of b. The approximate value obtained in this manner is

$$b \cong 1.73 \tag{5-60}$$

Thus a solution of Eq. 5-55 is of the form $\alpha = xC \cosh 1.73y$. A more general x variation could also be studied. If these loadings are used on a wing of finite aspect ratio, the drag in the middle section will be zero although the tip sections will have drag. Where there is no tip effect the total lift generated by each strip is zero whereas the lift per unit span is not zero. As a curiosity, one may find a loading for a wing of infinite aspect ratio which has zero drag but positive lift per unit span. However, if the wing is cut off, the tip sections will of course have drag. Among the many possible loadings which satisfy Eq. 5-55 in the middle section the optimal loading is the one which also satisfies Eq. 5-56 in the tip section. This idea may possibly be utilized for finding loadings of low drag although no computations of this nature have been carried out.

We shall now show that the drag of the optimal distribution cannot lie appreciably below the drag of the distributions discussed above. By a rather simple procedure, due essentially to R. Struble, one may construct a lower bound for the drag at given lift, i.e., an upper bound for ℓ.

As above, let α_B be the optimum within the restricted class C of loadings such that the angle of attack is odd in x. Denote the forward half of the planform ($-1 \leq x \leq 0$) by S_1 and the aft half ($0 \leq x \leq 1$) by S_2. Let α be the special loading in C such that $\alpha = -1$ on S_1 and $\alpha = +1$ on S_2. If p and L are the pressure and lift respectively of α it follows from Eq. 3-14 that

$$L = \frac{L_B}{2D_B}(\alpha,\alpha_B) = \frac{L_B}{D_B}\int_S \alpha p_B \, dS = \frac{L_B}{D_B}\left[\int_S p_B \alpha dS - 2\int_{S_1} p_B \, dS\right] \tag{5-61}$$

or

$$D_B = \frac{L_B^2}{L}\left[1 - \frac{2A}{L_B}\right] \tag{5-62}$$

where

$$A = \int_{S_1} p_B \, dS$$

To fix the ideas let us assume L_B to be positive. Since α_B is odd in x, it may be considered as a sum of a pair of deflected elements of opposite signs at (-x,y) and (x,y). Since the losses due to edge effects are greater for the forward one of the two elements in a pair it follows that the forward elements have predominately negative deflection for L_B positive. This makes it plausible that A as defined above is negative. This estimate is borne out by the optimal distributions for restricted classes, as constructed above (Eq. 5-13, 5-34, 5-47a, 5-54a). Hence, Eq. 5-62 implies

$$D_B \geq \frac{L_B^2}{L} \tag{5-63}$$

By linearized wing theory $L = 4q = \frac{qS}{AR}$

Hence,

$$\ell_B = \frac{L_B^2}{D_B q S} = \frac{1}{AR}\left(1 - \frac{2A}{L_B}\right)^{-1} \leq \frac{1}{AR} \tag{5-64}$$

and, cf. Eq. 5-16,

$$\ell_{OPT} = \ell_f + \ell_B = 4\left(1 - \frac{1}{2AR}\right) + \frac{4}{4AR}\left(1 - \frac{2A}{L_B}\right)^{-1} \leq 4\left(1 - \frac{1}{2(2AR)}\right) \tag{5-65}$$

Comparing this again with Eq. 5-16 it follows that

$$\ell_{OPT}(AR) \leq \ell_f(2AR) \tag{5-66a}$$

or

$$\frac{\ell_{opt}}{\ell_f} \leq \frac{4AR-1}{4AR-2} \tag{5-66b}$$

Thus the optimal ℓ for a rectangular wing with aspect ratio AR can never exceed the ℓ of a flat plate rectangle with aspect ratio 2AR. A lower bound for d_{opt} is then

$$\frac{d_{opt}(AR)}{d_f(AR)} \geq \frac{\ell_f(AR)}{\ell_f(2AR)} = \frac{1-\frac{1}{2AR}}{1-\frac{1}{4AR}} = \frac{4AR-2}{4AR-1} \tag{5-67}$$

Thus $\frac{d_{opt}}{d_f} \geq \frac{6}{7}$ for AR = 2 and $\frac{d_{opt}}{d_f} \geq \frac{14}{15}$ for AR = 4.

This formula shows that substantial drag savings are not possible for rectangular wings. Furthermore, it should be remembered that the lower bound for the drag was obtained by rather crude methods, and hence, may be somewhat lower than the actual minimum drag. The maximum values of ℓ actually obtained for the rectangular wing are plotted in Fig.5.7 on the same graph as the upper bound for ℓ.

The results obtained for the rectangular wing may be summarized as follows: Loadings of low drag have been constructed which have parabolic camber, $\alpha = xf(y)$, where $f(y)$ is a step function. The best result obtained for $AR \geq 3$ is the loading α_5 (Eq. 5-34) which has no camber in the middle section. For $AR \geq 3.05$ there is a slight improvement if the loading α_9 (Eq. 5-54a) is used; in this case part of the middle section has no camber, a narrow strip at each side of the middle section has negative camber, and the tips have positive camber, for positive lift. For $2 \leq AR \leq 3$, the best loading examined is α_8 (Eq. 5-49) in which the entire middle section has negative and the tips positive camber for positive lift. For $1 \leq AR \leq 2$, the loading α_1 (Eq. 5-14) has no spanwise variation in camber. It is believed that the choice of parabolic camber is quite good. Some further improvement may be obtained by allowing for greater y-variation in particular in the tip section. It seems plausible that the camber should increase

OPTIMUM ℓ AS A FUNCTION OF ASPECT RATIO FOR A RECTANGULAR WING

$M = \sqrt{2}$

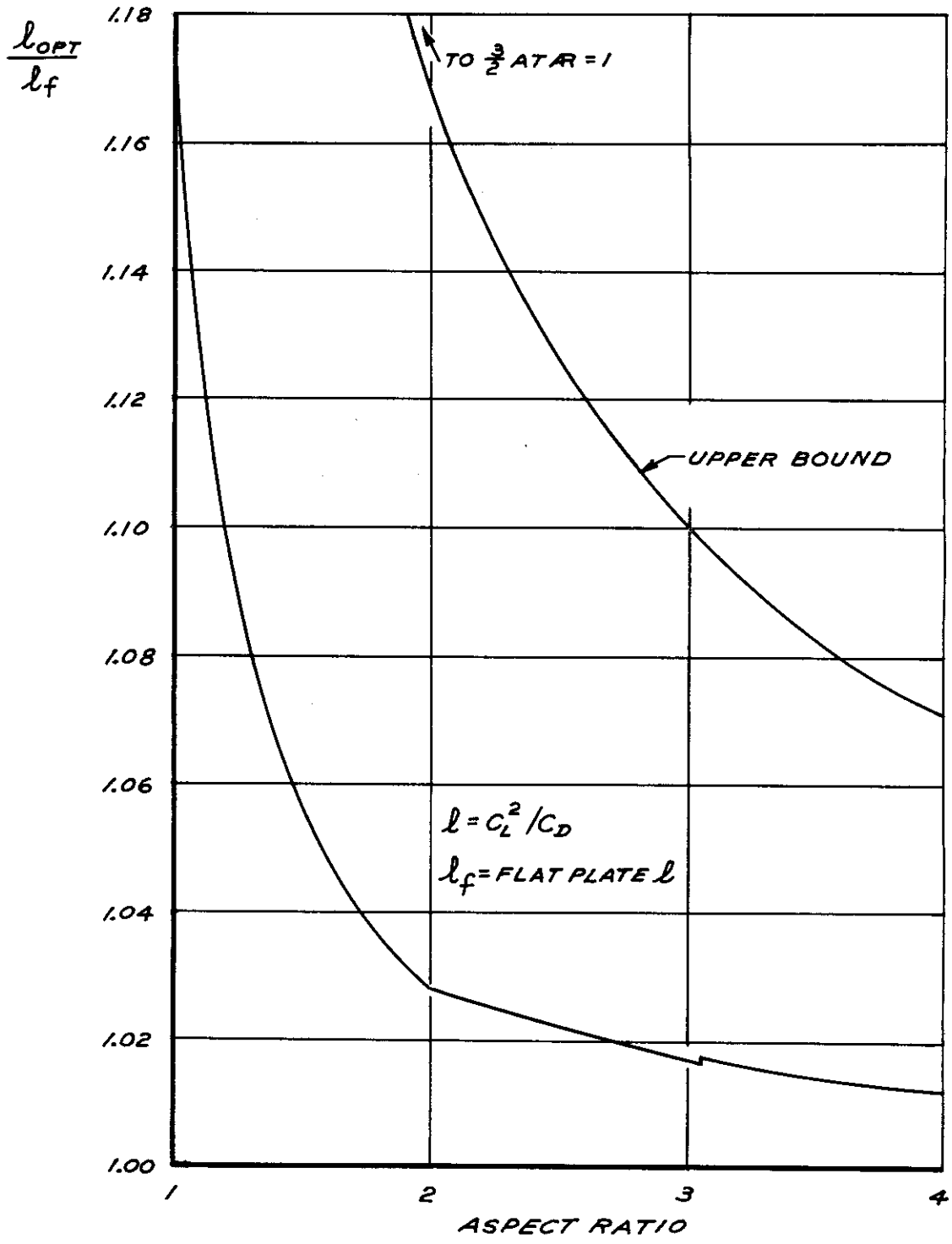

FIGURE 5-7

towards the side edges. The corresponding computations are quite straight forward in principle although they may be lengthy. The discussion in the present section was based on rather short calculations and was meant to establish certain general trends. As will be discussed in Chapter V the fuselage interference is of great importance in most practical problems, and hence, it seems unwarranted to make lengthy computations for wings alone.

Some typical numerical results are set forth in the table below and in the graph, Fig. 5.7.

COMPARISON OF OPTIMUM ℓ FOR RECTANGULAR WINGS WITH VARIOUS ASPECT RATIOS

AR	ℓ_f (AR≥1)	$\ell_{1_{OPT}}$ (AR≥1)	$\ell_{5_{opt}}=\ell_{3_{opt}}$ (AR≥3)	$\ell_{8_{opt}}$ (2≤AR≤3)	$\ell_{9_{opt}}$ (AR≥3.05)	ℓ_{opt}/ℓ_f
1.0	2.000	2.333	--	--	--	1.167
1.5	2.667	2.815	--	--	--	1.056
2.0	3.000	3.083	--	3.083	--	1.028
2.5	3.200	3.253	--	3.269	--	1.022
3.0	3.333	3.370	3.389	3.389	--	1.0167
3.05	3.344	3.380	3.399	--	3.401	1.0170
3.1	3.355	3.387	3.409	--	3.411	1.0167
3.5	3.428	3.456	3.476	--	3.478	1.014
4.0	3.500	3.521	3.542	--	3.543	1.012

6. REFERENCES

1. Jones, R. T., "The Minimum Drag of Thin Wings in Frictionless Flow," Journal of the Aeronautical Sciences, Vol. 18, No. 2, p. 75, February 1951.

2. Graham, E. W., "A Drag Reduction Method for Wings of Fixed Planform," Journal of the Aeronautical Sciences, Vol. 19, No. 12, p. 823, December 1952. Originally Douglas Aircraft Company Report No. SM-14441, July 15, 1952.

3. Rodriguez, A. M., Lagerstrom, P. A., and Graham, E. W., "Theorems Concerning the Drag Reduction of Wings of Fixed Planform," Journal of the Aeronautical Sciences, Vol. 21, No. 1, p. 1, January 1954. Originally Douglas Aircraft Company Report No. SM-14445, March 20, 1953.

4. Jones, R. T., "Theoretical Determination of Minimum Drag of Airfoils at Supersonic Speeds," Journal of the Aeronautical Sciences, Vol. 19, No. 12, p. 813, December 1952.

5. Walker, K., "Examples of Drag Reduction for Rectangular Wings," Douglas Aircraft Company Report No. SM-14446, January 15, 1953.

6. Beane, Beverly J., "Examples of Drag Reduction for Delta Wings," Douglas Aircraft Company Report No. SM-14447, January 12, 1953.

7. Tsien, S. H., "The Supersonic Conical Wing of Minimum Drag," Thesis, Cornell University, Graduate School of Aeronautics, June 1953.

8. Rott, N., "Minimum Drag Cambered Rectangular Wing for Supersonic Speeds," Journal of the Aeronautical Sciences, Readers' Forum, Vol. 20, No. 9, p. 642, September 1953.

9. Lagerstrom, P. A. and Van Dyke, M. D., "General Considerations About Planar and Non-Planar Lifting Systems," Douglas Aircraft Company Report No. SM-13432, June 1949.

10. Sedney, R., Unpublished Douglas Aircraft Company Memorandum.

11. Lagerstrom, P. A. and Graham, M. A., "Linearized Theory of Supersonic Control Surfaces," Douglas Aircraft Company Report No. SM-13060, July 1947.

A P P E N D I X

TABLE 1

VALUES OF $A_{\rho,\sigma}$

σ \ ρ	0	1	2	3	4	5	6
-6	-.181 818	.180034					
-5	.222222	-.233 766	.263248				
-4	-.285 714	.311 111	-.389 610	.789 743			
-3	.400 000	-.476 190	.933 333	.389 610	.263 248		
-2	-.666 667	1.200000	.476 190	.311 111	.233 766	.188 034	
-1	2.000 000	.666 667	.400000	.285 714	.222 222	.181 818	.153 846
0	2.000000	.666 667	.400 000	.285 714	.222 222	.181 818	.153 846
1	-.666 667	1.200 000	.476 190	.311 111	.233766	.188 034	.157576
2	.400000	-.476 190	.933 333	.389 610	.263 248	.202 597	.165 913
3	-.285 714	.311 111	-.389 610	.789 743	.337 662	.232 278	.181 271
4	.222 222	-.233 766	.263248	-.337 662	.696 832	.302 118	.210 157
5	-.181 818	.188 034	-.202 597	.232 278	-.302 119	.630467	.275 847
6	.153 846	-.157 576	.165 913	-.181 271	.210 156	-.275 848	.580030
7	-.133 333	.135 747	-.140 989	.150 112	-.165509	.193344	-.255415
8	.117 647	-.119 298	.122 819	-.128 730	.138 104	-.153 249	
9	-.105 263	.106 443	-.108 925	.112 994	-.119 194		
10	.095238	-096 110	.097 928	-.100 856			
11	-.086 957	087 619	-.088 990				
12	.080 000	-.080 515					

TABLE 2

VALUES OF $B_{\rho,\sigma}$

σ \ ρ	0	1	2	3	4	5	6
0	1.333333	-.266 667	-.038 095	-.012 698	-.005 772	-.003108	-.001 865
1	.800000	.571 428	-.266 667	-.051 948	-.020513	-.010390	-.006 034
2	-.190 476	.444 444	.432 900	-.239 316	-.051 948	-.022 122	-.011 848
3	.088 889	-.121 212	.335043	.363636	-.216 792	-.049 760	-.022 122
4	-.051 948	.061 538	-.093 506	.278 732	.319 890	-.199094	-.047 288
5	.034 188	-.038 095	.048 668	-.078 196	.243338	.288 983	-.184 936
6	-.024242	.026 144	-.030804	.041 083	-.068 305	.218 562	.265 631

TABLE 3

INTERFERENCE DRAG BETWEEN ANGLE OF ATTACK

DISTRIBUTIONS $OC_{m,n}$ AND $OC_{p,g}$, $D_{m,n;p,g}$

M \ N	0				1				2			
	g \ p	0	1	2	3	0	1	2	3	0	1	2	3
0	0	18.692 064	-1.246 136	-.251 955	-.130 360	3.718 708	.936 212	-.930 671	-.429 520	2.354 738	.387 418	.747 663	-.685 209
	1	3.718 708	-.401 773	-.084 525	-.046 556	9.313 137	.074 531	-.049 206	.026 514	2.389 470	-.062 843	.057 893	-.078 665
	2	2.354 738	-.209 520	-.030 599	-.013 910	2.389 470	-.014 230	-.076 806	-.021 320	7.154 364	-.096 602	.057 280	-.008 385
1	g \ p	0	1	2	3	0	1	2	3	0	1	2	3
	0	-1.246 136	2.930 637	.493 680	.349 788	-.401 773	-.373 197	.295 772	.112 062	-.209 520	-.056 542	-.322 035	.252 045
	1	.936 212	-.373 197	-.173 148	-.095 488	.074 531	1.233 255	-.182 062	-.025 280	-.014 230	.199 173	.150 356	-.171 865
	2	.387 418	-.056 542	-.042 278	-.016 998	-.062 843	.199 173	-.096 424	-.025 377	-.096 601	.647 186	.049 472	-.014 094
2	g \ p	0	1	2	3	0	1	2	3	0	1	2	3
	0	-.251 955	.493 680	1.428 629	.282 178	-.084 525	-.173 148	.068 320	-.026 364	-.030 599	-.042 278	-.023 736	.032 804
	1	-.930 671	.295 770	.068 320	.002 284	-.049 206	-.182 062	.681 473	.107 590	-.076 806	-.096 424	-.108 191	.092 044
	2	.747 663	-.322 035	-.023 736	-.046 475	.057 893	.150 356	-.108 191	-.061 433	.057 281	.049 472	.432 657	-.071 785
3	g \ p	0	1	2	3	0	1	2	3	0	1	2	3
	0	-.130 360	.349 788	.282 178	1.085 083	-.046 556	-.095 488	.002 284	-.022 595	-.013 910	-.016 998	-.046 475	.040 298
	1	-.429 520	.112 062	-.026 364	-.022 595	.026 514	-.025 280	.107 590	.379 312	-.021 320	-.025 377	-.061 433	.036 338
	2	-.685 209	.252 045	.032 804	.040 298	-.078 665	-.171 865	.092 044	.036 338	-.008 385	-.014 094	-.071 784	.299 166

TABLE 4

LIFT CORRESPONDING TO ANGLE OF ATTACK DISTRIBUTION $\alpha_{m,n}$

$L(\alpha_{m,n})$

m \ n	0	1	2
0	2.844 444	3.982 222	2.969 475
1	-1.760 846	-0.297 989	-0.171 173
2	-0.908 744	-0.090 136	-0.039 376
3	-0.627 994	-0.051 717	-0.019 079

CHAPTER III

SPATIAL LIFT DISTRIBUTIONS

by

E. W. Graham
B. J. Beane
R. M. Licher

1. SUMMARY

A preliminary study is made of non-planar wing systems (biplanes, multiplanes, etc.) for use in supersonic flight. Such arrangements offer the possibility of aerodynamic or structural improvements over monoplanes, and so require investigation.

This study is general in that lift distributions throughout volumes of prescribed shape are considered without detailed analysis of the wing systems required to support the lift. The restriction of the location of lifting elements to a given volume is necessary to insure that the aerodynamic optimum is structurally feasible.

For ellipsoidal volumes and other special shapes the optimum distributions of lift are found, and (for some cases) minimum drag values are obtained. (The optimum lift distribution is defined as that which gives minimum possible wave plus vortex drag for any wing system contained within the volume and supporting a given lift.) For special cases the necessary wing areas are determined.

For planar wings the drag due to thickness and drag due to lift are separable. This is not generally true for distributions in three dimensions. Such interference problems are discussed, and it is shown that, in some cases, there is no interference drag between thickness distributions and the optimum distribution of lifting elements alone.

For planar wings the optimum distribution of lift is generally unique. For lift distributions in space the optimum is not generally unique. This suggests such problems as determining which of the optimum distributions can be supported on the least wing area.

2. INTRODUCTION

Much attention has been devoted to the study of planar wings (monoplanes) for use in supersonic flight. Many different planforms have been studied using linearized theory, and the problems of determining drag due to lift and drag due to thickness have been investigated. These investigations have led to searches for "optimum" pressure distributions (those giving minimum drag for a given lift or minimum drag for a given frontal area, etc.).

Such studies should be extended to include non-planar wing systems (biplanes and multiplanes), which offer the possibility of aerodynamic and structural improvements. The reduction of drag due to thickness by the Busemann biplane effect is one possible advantage. The reduction of wave drag due to lift by more efficient distribution of lifting elements may be possible. Reductions of vortex drag are obtained in multiplane systems without increasing the span. Also the increased depth available may make external structure useful if drag penalties are not too large.

One possible approach to the study of non-planar systems is to choose and analyze specific multiplane arrangements, and make comparisons with planar systems. A second approach, which is somewhat more general in nature, is to study distributions of lift through a given volume, and attempt to determine optimum distributions. The latter procedure is adopted here.

In studying lift distributions through a volume of prescribed shape, the detailed structure of the wing system and its viscous and thickness drag are temporarily neglected. The optimum distribution is then one which gives the least possible wave plus vortex drag for any wing system contained within the prescribed volume.

The most obvious application of such a study is to the design of airplanes or missiles having some "compactness" requirement (for example, where a missile must be stowed within a given space). However, the volume restriction also introduces a primitive control of structural weight. The necessity for such a control can be seen as follows. The vortex (or "induced") drag of a wing is inversely proportional to the square of the span. This means that the aerodynamically desirable wing is one of infinite span and, therefore, structurally impossible. Similarly the wave drag of a wing is inversely proportional to the squares of certain projected dimensions of the wing, and the aerodynamic optimum again requires infinite dimensions for the wing.

In order to make the aerodynamically optimum wings structurally possible it is necessary to apply some dimensional limitations. A limit on wing area is not sufficient, since the trend is then towards infinite aspect ratio wings swept behind the Mach cone. (For example see Ref. 1.) Another possibility is the restriction of lifting elements to a volume of prescribed shape, and this is the restriction applied in this report. Its application may be regarded as a first concession to the importance of structural problems.

Another factor which must be considered in studying lift distributions through volumes is the wing area required to support the lift. If this area is infinite the viscous drag becomes infinite. However, the minimum value of wave plus vortex drag can be obtained with finite wing areas in many (and possibly all) instances.

3. INTERFERENCE EFFECTS

For the planar wing there is no interference between the drag due to lift and drag due to thickness. This corresponds to the fact that a source and lifting element have no interference drag if the axis of the lifting element is normal to the plane containing the source, the lifting element and the free stream direction. This was shown by Hayes[2]. The lifting element is the elementary horseshoe vortex, and its axis is defined to be in the direction of the force produced.

However, for general distributions of sources and lifting elements in space there is interference drag. An example of this is the reduction of drag due to lift by the insertion of a thickness distribution in the pressure field of a lifting wing (see Appendix III-A).

Although in general such interference effects exist it can be shown (see Appendix III B) for many volumes that the interference disappears when the optimum distribution of lifting elements alone has been attained. This means that such an optimum cannot be further improved by introducing a thickness distribution. For this reason the minimum drag values obtained by studying lifting elements alone are significant.

A complete study of non-planar wing systems should include those in which side forces are developed (for example, "ring" wings) since side forces and lift forces may produce interference drag. This part of the investigation will be undertaken later.

In the following discussion it will also be assumed that the wing system is isolated, and so does not feel interference effects from the ground or from any other wing system.

4. METHODS FOR EVALUATING SUPERSONIC WING DRAG

The non-viscous drag of a wing moving at supersonic speeds may be obtained from two different points of view[2] using linearized theory. First, the drag may be evaluated by integrating the local pressure times local angle of attack over the wing surface. Second, the drag can be evaluated from momentum (and energy) considerations involving the flow field at a great distance from the wing. In the latter case part of the drag is associated with the production of kinetic energy in the trailing vortex system, and is called vortex drag. This drag is identical with that produced by the same spanwise lift distribution in an incompressible flow (frequently called "induced" drag). The remainder of the drag is associated with the production of kinetic and potential energy near the surface of the Mach cone whose vertex is the wing system. This is called wave drag. The wave drag plus the vortex drag is equal to the drag evaluated at the wing surface by the first method.

5. THE "COMBINED FLOW FIELD" CONCEPT

The idea of the "combined flow field" was introduced by Munk[3] and extended by R. T. Jones[1,4]. Consider a distribution of lifting elements in a free stream of given velocity. A certain downwash velocity and pressure are produced at each point in the field. If the direction of the free stream is now reversed without moving the lifting elements or altering their intensities, then in general different downwash velocities and pressures are produced at each point in the field. The sum of the downwash velocities produced in the forward and the reverse flows is called the downwash velocity of the combined flow field. The difference of the pressures in the foward and reverse flows is called the pressure in the combined flow field.

It should be remembered that in the flow reversal the lift distribution is kept fixed, not the geometry, i.e., angle of attack distribution, of the wing.

6. CRITERIA FOR IDENTIFYING OPTIMUM LIFT DISTRIBUTIONS

A necessary and sufficient condition for minimum wave plus vortex drag was given by R. T. Jones[4] in connection with planar systems. The condition is that the downwash in the combined flow field shall be constant at all points of the planform. This result depends on the fact that a pair of lifting elements has the same drag in forward and reverse flow, which is also true when the lifting elements are not in the same horizontal plane. Hence, the above criterion can be extended immediately to lift distributions in a volume by requiring constant downwash (in the combined flow field) throughout the volume.

A necessary and sufficient condition for vortex drag alone to be a minimum is that the downwash velocity throughout the wake of the wing system shall be constant far behind the wing (the wake is defined as the projection of the lifting regions on the Trefftz plane). This condition was given by Munk[5].

In special cases elliptic loadings identify minimum wave drag configurations, as has been shown by Jones[1]. Such a criterion can also be derived from Hayes' method[2]. The loadings for the latter method are obtained as follows. Let the lifting volume be cut by a set of parallel planes each inclined at the Mach angle to the flow axis (see Fig. 1). Place all the lift intensity cut by any one plane at the intersection of the plane with the flow axis. When this has been done for each plane in the set a load distribution is obtained. If a second set of parallel planes is used a second loading is obtained, etc. If the loadings are elliptical for all possible sets of parallel planes inclined at the Mach angle, then the wave drag is

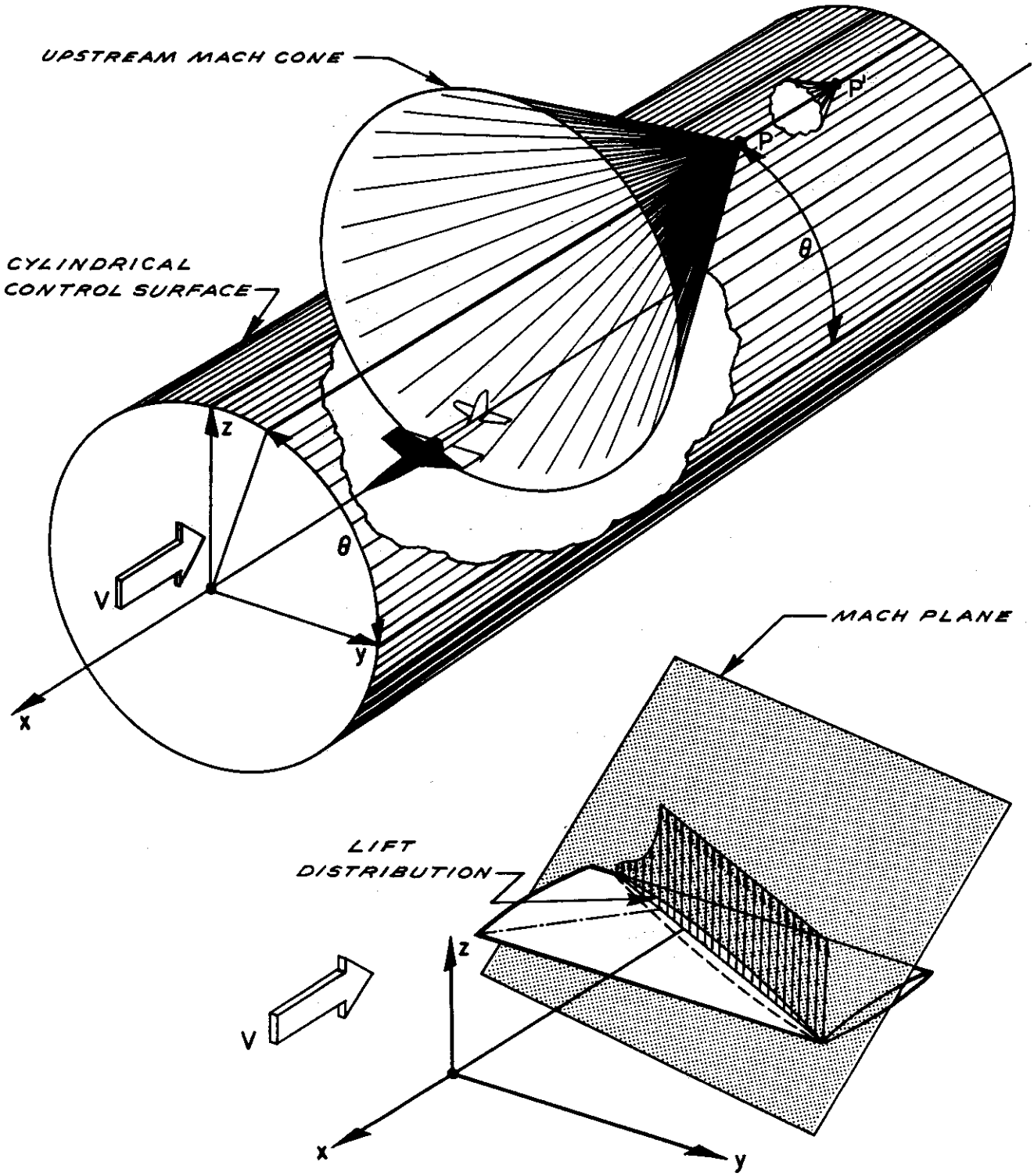

GEOMETRY INVOLVED IN EVALUATION OF WAVE DRAG DUE TO LIFT

FIGURE 1

a minimum. In Hayes' procedure for calculating drag this condition corresponds to obtaining the minimum possible drag contribution at <u>every</u> angular position on the cylindrical control surface. Such minima cannot be attained in general, but if they are attained and if the vortex drag is also a minimum then the more general criterion (constant downwash in the combined flow field) is satisfied.

If the wake of the wing system has an elliptical cross-section and is symmetrical right to left, then a constant intensity of lift over the cross-section gives the minimum possible vortex drag. Munk[5] gave this criterion for a circular cross-section, and his method can be used to obtain the generalization indicated. In particular, when the cross-section of the wing wake degenerates into a horizontal line, (corresponding to a planar wing) the familiar requirement of elliptic spanwise load distribution is obtained. The general requirement of constant downwash in the wing wake (far behind the wing) is satisfied by the above lift distributions.

7. THE OPTIMUM DISTRIBUTION OF LIFT THROUGH A SPHERICAL VOLUME

Consider a sphere of radius "a" with its center at the origin, and let a total lift "L" be distributed through the sphere with local intensity "ℓ". If $\ell = \frac{L}{\pi^2 a^2 \sqrt{a^2-r^2}}$, r being the radial distance from the origin, then elliptic loadings are obtained when the sphere is cut by any set of parallel planes. The fact that elliptic loadings are produced when the planes are inclined at the Mach angle (to the free stream direction) insures that the wave drag is a minimum. The cross-section of the wake is circular, and if the lift intensity is projected onto a plane normal to the free stream direction it can be shown that the lift is uniformly distributed over this circular cross-section. This insures that the vortex drag is also a minimum.

The lift distribution $\ell = \frac{L}{\pi^2 a^2 \sqrt{a^2-r^2}}$ then gives the minimum possible wave and vortex drag. By Hayes' procedure it can be found that the minimum wave drag is $D_{\text{min wave}} = \frac{L^2 (M^2-1)}{2\pi q (2a)^2 M^2}$, the minimum vortex drag[5] is $D_{\text{min vortex}} = \frac{1}{2}\left(\frac{L^2}{\pi q (2a)^2}\right)$ and the minimum total drag is $D_{MIN} = \frac{1}{2}\frac{L^2}{\pi q (2a)^2}\left[\frac{2M^2-1}{M^2}\right]$

The largest planar wing of circular planform contained in the sphere has a minimum drag[1] which is greater by the ratio $\frac{2M^3}{2M^2-1}$. This is a factor of 1.885 at $M = \sqrt{2}$. However the wing area required to obtain minimum drag for the spherical volume is not yet determined and the drag comparison is of course not complete without consideration of the viscous drag (and thickness drag).

8. THE OPTIMUM DISTRIBUTION OF LIFT THROUGH AN ELLIPSOIDAL VOLUME

The spherical volume with its optimum lift distribution can be changed into an ellipsoidal volume with a corresponding lift distribution by a scale transformation of one of the Cartesian coordinates. This transformation transforms planes into planes so that elliptical loadings are preserved for the ellipsoid and minimum wave drag is obtained. Also, a constant intensity of lift over the wake cross-section is maintained for the ellipsoid, and if this cross-section is symmetrical right to left, then the vortex drag is also a minimum. Although the optimum lift distribution for an ellipsoid is obtainable from the spherical case, the value of the minimum drag is not necessarily the same. (Minimum drag values for ellipsoids will be given in a later report.)

In one limiting case an ellipsoid is collapsed into a horizontal planar wing of elliptic planform carrying constant pressure. Optimum cases of this type were first discussed by R. T. Jones[1]. Another limiting case which gives minimum drag occurs when an ellipsoid is collapsed into a plane normal to the flow direction. Then the wing system can be interpreted as a uniformly loaded airfoil cascade (of zero chord and gap) within the elliptical cross-section. The entire cascade can be analyzed as a two-dimensional system.

If the chord is chosen to be $\sqrt{M^2-1}$ times the gap then the airfoils in the cascade are non-interfering, but the lift distribution is sufficiently continuous (see illustration). In other words, when the cascade is cut by planes inclined at the Mach angle, the resulting load distributions used in Hayes' method will be continuous. The total wing

area is then $\sqrt{M^2-1}$ times the area of the ellipse.

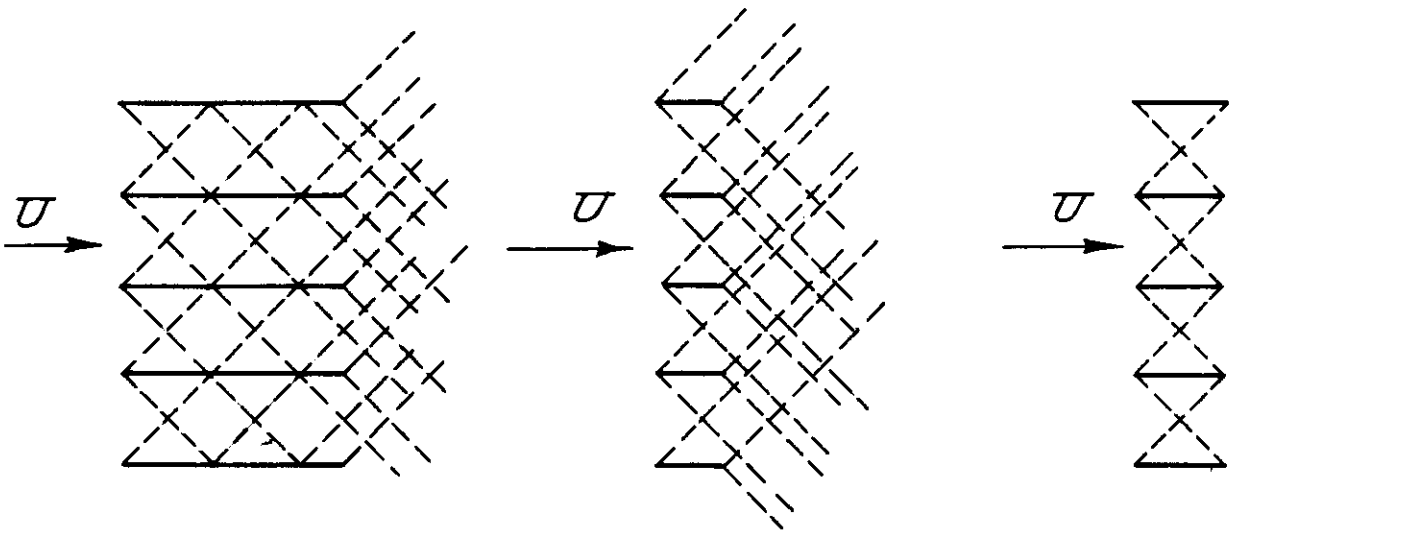

INTERFERING AIRFOILS

NON-INTERFERING AIRFOILS

NON-INTERFERING AIRFOILS WITH SUFFICIENTLY CONTINUOUS LIFT DISTRIBUTION

9. THE OPTIMUM DISTRIBUTION OF LIFT THROUGH A "DOUBLE MACH CONE"

Consider a volume consisting of two Mach cones placed base to base. If a uniformly loaded cascade of airfoils (with zero gap and chord) is placed at the maximum cross-section of this volume then elliptic loadings will be obtained when the volume is cut by planes inclined at the Mach angle. This airfoil cascade consequently produces the minimum possible wave drag for wing systems contained within the volume and carrying a specified lift. The uniform distribution of load over the circular cross-section insures minimum vortex drag also, so the lift distribution is an optimum for the double Mach cone.

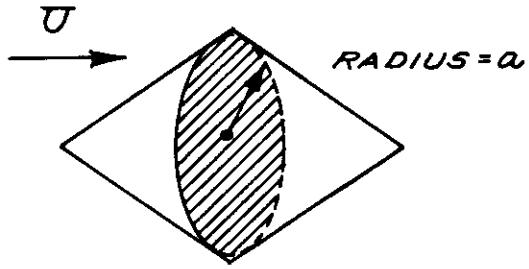

The value of the minimum wave drag (obtained by Hayes' method) is $D_{wave} = \frac{1}{2}\frac{L^2}{\pi q (2a)^2}$ and the vortex drag has the same magnitude in this case.

The wave plus vortex drag is then $D = \frac{L^2}{\pi q (2a)^2}$. This is equal to the minimum vortex drag <u>alone</u> for a planar wing of span 2a. If the airfoil cascade is compared to the largest planar wing of diamond planform which can be contained within the double Mach cone, the minimum wave plus vortex drag of the diamond planform is approximately 1.52 times greater than for the cascade. (See Chapter II for analysis of the diamond planform.)

Again it must be emphasized that the drag comparison is not complete without the inclusion of viscous drag and thickness drag for the wing system.

Since the circular cascade is an optimum arrangement it satisfies Jones' downwash criterion; this can be checked as follows. By two-dimensional analysis it can be shown that the downwash, ϵ, in the aft Mach cone is 2α, where α = the angle of attack of each airfoil. Since the downwash is zero in the fore Mach cone, the downwash in the combined flow is then constant and equal to 2α throughout the double Mach cone. (Far behind the cascade in the wake of the wing system $\epsilon = \alpha$. This can be shown by equating lift to rate of change of vertical momentum.)

10. NON-UNIQUENESS OF OPTIMUM LIFT DISTRIBUTIONS

In incompressible flow an elliptic spanwise lift distribution insures the minimum possible drag due to lift. According to Munk's stagger theorem[5] the chordwise location of the lifting elements is unimportant so there are infinitely many distributions of lift over a given planform which produce the minimum drag.

In supersonic flow this non-uniqueness of optimum distributions still persists. For example the minimum wave drag for a double Mach cone volume can be attained with each of three different simple lift distributions. The first is a constant intensity over the circular disc at the maximum cross-section of the volume. The second is an elliptical intensity concentrated on the axis of the volume. The third is a constant intensity throughout the entire double Mach cone. If the first two distributions are superimposed, one carrying a unit of positive lift and the other a unit of negative lift, the result is a net lift equal to zero. Also the net strength of the lifting elements intercepted by any cutting plane inclined at the Mach angle is zero. This means that the combined distribution has zero wave drag. Furthermore, there are no disturbances whatsoever produced far out on the Mach cone and no wave drag interference can exist with any other loading. If another such combined distribution with opposite sign is placed on the same streamwise line with the first one, then,by Munk's stagger theorem, the vortex drag is zero also. This may be called a "zero loading" (see illustration).

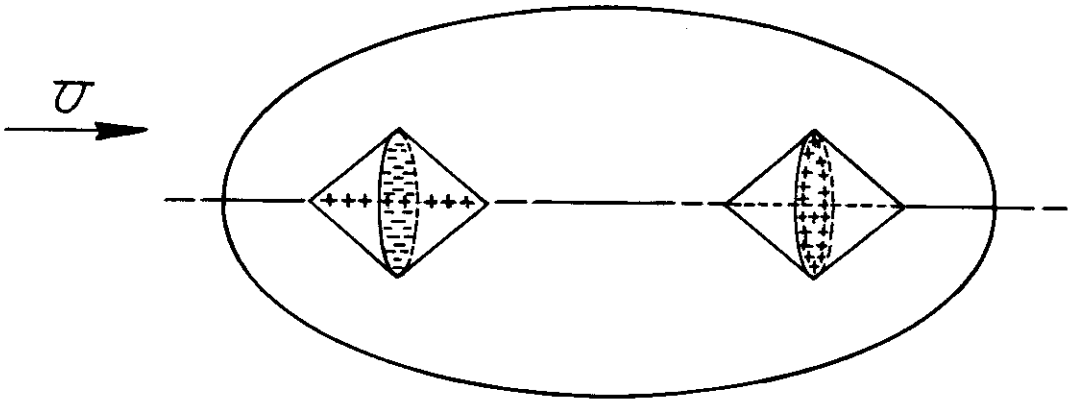

A "Zero Loading" Placed Within an Ellipsoidal Volume

Such a "zero loading" placed within any volume alters neither the lift nor the drag of the original lift distribution. For this reason optimum lift distributions in three dimensions are never unique (unless the volume degenerates into a surface).

In incompressible flow the infinitely many optimum lift distributions over a planform (all of which produce elliptic spanwise loading) are indistinguishable as regards the vortex pattern produced far behind the wing. This is also true in supersonic flow and in addition the optimum lift distributions for a given volume are indistinguishable in their effects far out on the Mach cone.

In view of the non-uniqueness of the optimal distributions, it is desirable to find that one which requires the minimum wing area, or is best adapted for structure.

11. REFERENCES

1. Jones, Robert T., "Theoretical Determination of the Minimum Drag of Airfoils at Supersonic Speeds," Jr. Aero. Sci. Vol. 19, No. 12, December, 1952.

2. Hayes, Wallace D., "Linearized Supersonic Flow," North American Aviation, Inc., Inglewood, Report No. A.L. 222, June 1947.

3. Munk, Max M., "The Reversal Theorem of Linearized Supersonic Airfoil Theory," Jr. Applied Physics, Vol. 21, No. 2, pp. 159-161, February 1950.

4. Jones, Robert T., "The Minimum Drag of Thin Wings in Frictionless Flow," Jr. Aero. Sci., Vol. 18, No. 2, pg. 75, February 1951.

5. Munk, Max M., "The Minimum Induced Drag of Airfoils," NACA TR 121, 1921.

APPENDIX III-A

REDUCTION OF DRAG DUE TO LIFT BY ADDITION OF A THICKNESS DISTRIBUTION

Consider the two-dimensional system sketched in the figure below. The cross-hatched area is a thickness distribution lying partly in the pressure field of a flat-plate wing. The relative geometries of the thickness distribution and the lifting surface are indicated in the figure. Also, the pressure distributions, relative to the two-dimensional pressure $2\alpha q/\beta$ are shown in parentheses.

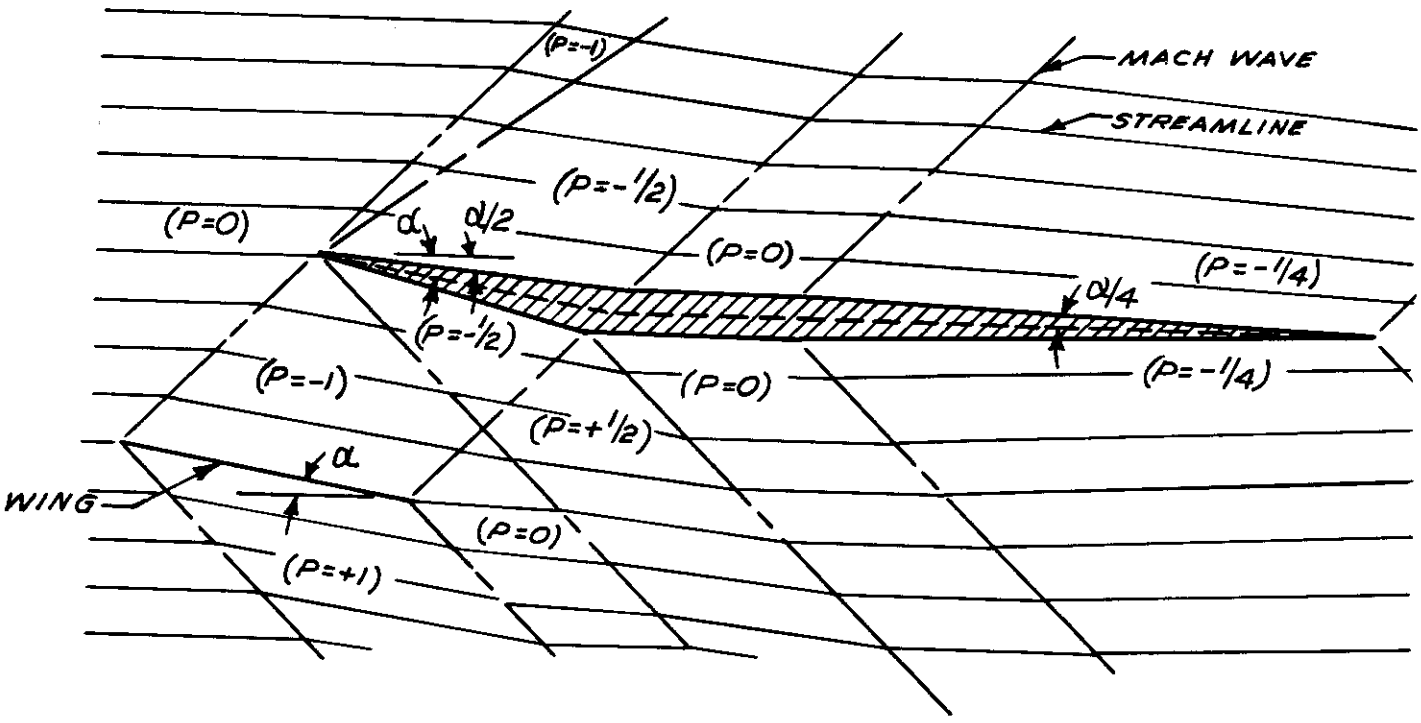

As long as the pressure field of the thickness distribution does not intersect the flat-plate, the lift of the system is the same as for the flat-plate by itself. On the other hand, the interference between the pressure field of the flat-plate and the thickness distribution produces

a negative drag contribution. In the example shown, negative drag is contributed by the pressure P = - 1/2 on the front part of the thickness and positive drag by the pressure P = -1/4 on the rear part of the thickness; the net drag contribution of the thickness, based on its frontal area, is - 1/4. For the flat plate, the drag is + 2 based on the same frontal area, and this drag is not influenced by the presence of the thickness distribution. Omitting friction, the total drag of the system (wing plus thickness) is 12-1/2 percent less than the drag of the flat-plate alone. Thus, the total lift in this case is unaffected by introduction of the thickness distribution and a drag reduction is obtained.

This example is similar to the Busemann biplane, and is consistent with the fact that in the general case (non-planar systems) sources and lifting elements have an interference drag.

APPENDIX III-B

THE NON-INTERFERENCE OF SOURCES WITH OPTIMUM DISTRIBUTIONS OF LIFTING ELEMENTS IN A SPHERICAL VOLUME

In general there is interference between non-planar distributions of sources and lifting elements, as shown by Hayes[2] (For an example see Appendix I.) This suggests that it might not be possible to separate the lift and thickness problems, so that the optimum distribution of lifting elements alone might not be significant.

It, therefore, becomes important to establish whether or not a single source placed within a volume has an interference drag with the optimum distribution of lifting elements alone in that volume.

Following is a proof that a single source placed at any point within a sphere has no interference drag with the optimum distribution of lifting elements alone in the sphere.

An optimum distribution of the total lift, L, within a sphere of radius "a" (center at the origin) is given by

$$\ell_{OPT} = \frac{L}{\pi^2 a^2} \frac{1}{\sqrt{a^2 - r^2}}$$

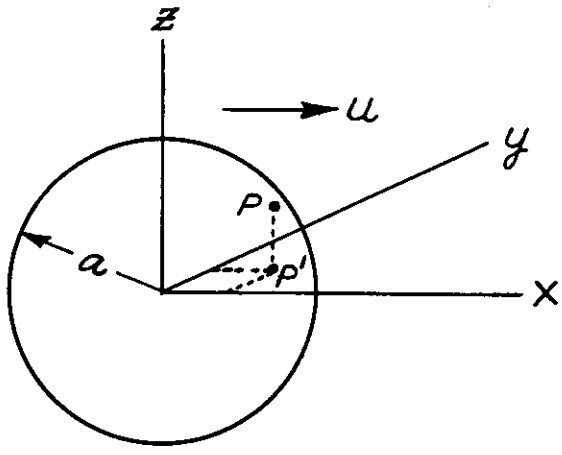

where r = spherical radius to any point. Let a source located at an arbitrary point, P, within the sphere be denoted by S, and let P' be the projection of P on the horizontal (x-y) plane. The potential of S is identical with that caused by some lifting element distribution, ℓ', on the line between P and P' plus a source S' at P'. (This follows from Appendix III-C.)

The distribution l' has zero net lift.

The interference between l_{opt} and S is equal to the interference between l_{opt} and S' plus the interference between l_{opt} and l'. The first component is zero because of the symmetry of l_{opt} about the x-y plane. That is, the interference drag between a downstream source in the x-y plane, for example, and two equal lift elements located symmetrically with respect to the x-y plane is due to the pressures induced at the source by the lifting elements. (See illustration.) These will be equal in magnitude and of opposite sign, so that the net interference drag is zero. Similarly, the interference drag between the lifting elements and an upstream source arises from the downwash velocities induced by the source at the lifting elements. These again are of equal magnitude and opposite sign and the interference drag is zero. If the interference between l_{opt} and l' were not also zero it would be possible to obtain a distribution of lifting elements alone with lower drag than l_{opt} Since l_{opt} has the minimum drag by definition, the second interference component is zero. This completes the proof for a <u>particular</u> l_{opt}.

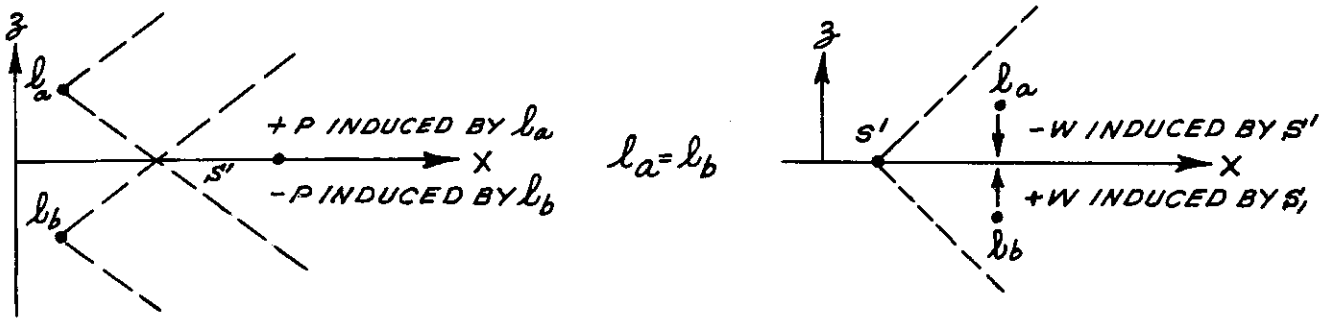

This proof can be extended to the entire family of optimum lift distributions in the sphere as follows. As previously mentioned, all of the optimum distributions produce identical effects far out on the Mach cone and far behind the wing system. Interference drag terms can be computed from these distant effects alone. Hence, a source has the same interference drag with

each of the optimum distributions, and this is zero for all cases since it has been proved zero for one case.

This proves that source distributions in a spherical volume cannot reduce the drag attained with any of the optimum distributions of lifting elements alone in that volume.

Similar methods may be applied to ellipsoids having one principal axis vertical, to double Mach cones, and to many other volumes. It is sufficient that the volume has a horizontal plane of symmetry, and that the vertical lines connecting all points in the volume with this plane are entirely contained within the volume.

APPENDIX III-C

INTERCHANGEABILITY OF SOURCE AND LIFTING ELEMENT DISTRIBUTIONS

The disturbance field of a unit source located at x_o, 0, z_o is represented by the velocity potential

$$\phi = -\frac{1}{2\pi\sqrt{(x-x_o)^2-y^2-(z-z_o)^2}}$$

and that of a unit lifting element by

$$\phi = \frac{1}{2\pi\rho V}\frac{(x-x_o)(z-z_o)}{\left[y^2+(z-z_o)^2\right]\sqrt{(x-x_o)^2-y^2-(z-z_o)^2}}$$

(Ref. 2)(Note that the unit lifting element is an elementary horseshoe vortex, the potential of which is obtained from the source potential by integrating axially and differentiating vertically. The factor ρV in the denominator of the above is introduced in order to define the strength of this singularity in terms of its lift rather than its circulation.)

Consider, first, lifting elements of constant strength (ρVK) distributed uniformly on a vertical line extending from z_1 to z_2. If this distribution of lifting elements is transferred in the free-stream direction from $x = x_1$ to $x = x_2$, the change in velocity potential is

$$\phi = \frac{K}{2\pi}\left[(x-x_2)\int_{z_1}^{z_2}\frac{(z-z_o)dz_o}{\left[y^2+(z-z_o)^2\right]\sqrt{(x-x_2)^2-y^2-(z-z_o)^2}}\right.$$

$$\left.-(x-x_1)\int_{z_1}^{z_2}\frac{(z-z_o)dz_o}{\left[y^2+(z-z_o)^2\right]\sqrt{(x-x_1)^2-y^2-(z-z_o)^2}}\right] \qquad (a)$$

Similarly, sources of constant strength (K) are considered to be distributed along a horizontal line extending from x_1 to x_2. The transfer of this source distribution vertically from $z = z_1$ to $z = z_2$ results in a change in velocity potential given by

$$\phi = -\frac{K}{2\pi}\left[\int_{x_1}^{x_2} \frac{dx_o}{\sqrt{(x-x_o)^2-y^2-(z-z_2)^2}} - \int_{x_1}^{x_2} \frac{dx_o}{\sqrt{(x-x_o)^2-y^2-(z-z_1)^2}}\right] \qquad (b)$$

Integration shows that ϕ is identical in these two cases. Thus, the source distribution (b) is equivalent to a transfer of lifting elements streamwise, while the lifting element distribution (a) is equivalent to a transfer of sources vertically. This derivation applies, of course, only to points whose upstream Mach cones contain the entire source and lifting element distributions. However, the proof can be extended to cover all points external to the area enclosed by the two lines of lifting elements and the two lines of sources.

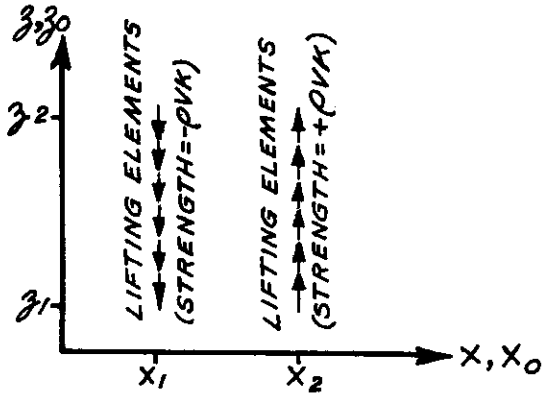

a) LIFTING ELEMENT DISTRIBUTION

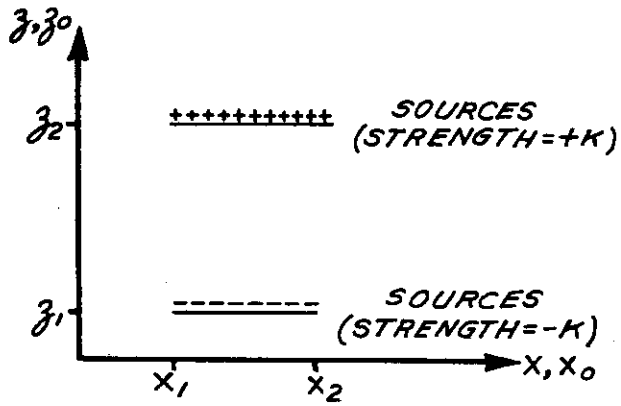

b) SOURCE DISTRIBUTION

$\phi_a = \phi_b$

Consider also the limiting case when the line of positive lifting elements (Fig. (a) above) and the line of negative lifting elements are allowed to approach one another while the product of lifting element strength and the distance separating the two lines retains a constant finite value. The velocity potential in this instance is the derivative of the velocity potential of a single line of lifting elements, and can be shown to be the same as the velocity potential due to a source and a sink located at the two ends of the lifting element distribution.

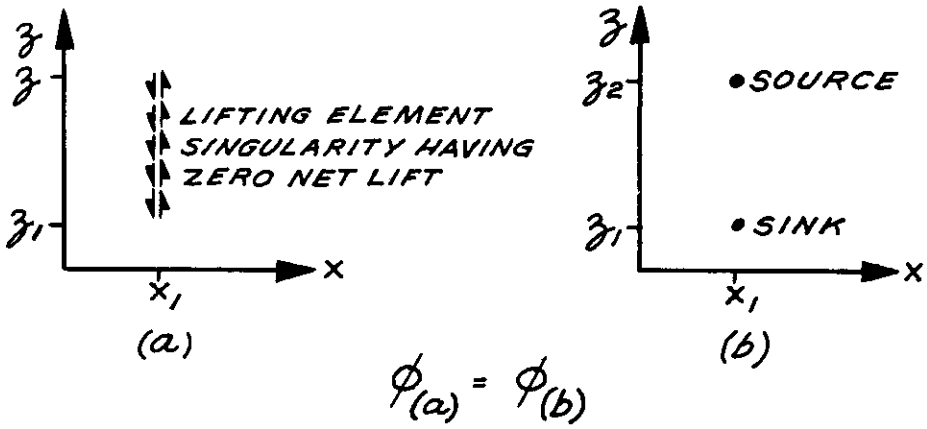

Thus, the singularity described can be used to transfer a single source vertically, as illustrated in the figure below.

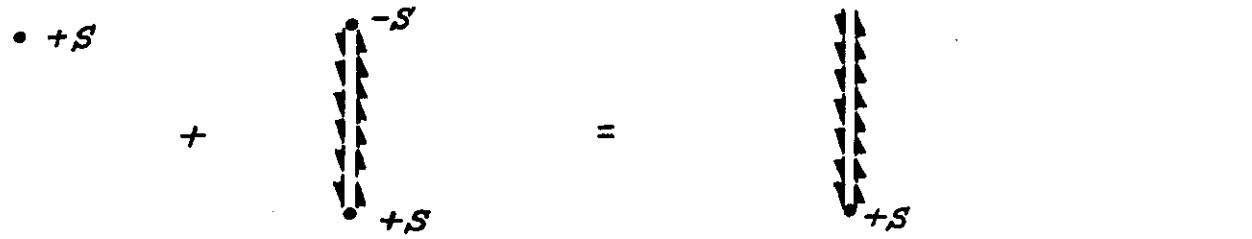

From these examples, it is evident that there is a certain interchangeability of source and lifting element distributions. Source distributions within the volume may have the effect of transferring lift in the free stream direction, and lift distributions may correspond to the vertical displacement of a source. In the first case the net source strength is zero. In the second case the net strength of the lifting elements is zero.

CHAPTER IV

BIPLANE LIFT DISTRIBUTIONS

by

E. W. Graham

and

R. M. Licher

1. SUMMARY

The use of biplanes for supersonic flight is investigated. Two types of biplanes are considered. The first is the Busemann biplane which makes use of interference effects between the upper and lower wings to eliminate (in large part) the thickness drag of the wings at the design Mach number. The second is the non-interfering biplane, each of whose wings acts as an isolated monoplane at and above the design Mach number.

Analyses made by other authors indicate that the Busemann biplane does not offer any obvious advantages over a monoplane arrangement for the design conditions now contemplated for supersonic flight.

For non-interfering biplanes, as compared to aerodynamically equivalent monoplanes, an inherent structural advantage appears. This advantage is the result of a scale effect for geometrically similar structures.

Such an advantage might be most fully realized for a supersonic missile launched from a supersonic aircraft. Here performance below the design Mach number might be unimportant.

A possible disadvantage of the "non-interfering" biplane is the transfer of lift from one wing to the other that may occur below the design Mach number.

Means for reducing this lift transfer (or its consequent structural penalties) are discussed, and more detailed study of some configurations is recommended.

2. INTRODUCTION

The use of biplanes for supersonic flight has been suggested many times. Busemann showed[1] that the thickness drag of an infinite aspect ratio biplane could be reduced essentially to zero at one prescribed Mach number by proper design of the airfoil sections. However, such a biplane must have twice the wing area of a monoplane supporting the same lift at the same angle of attack or must operate at twice the angle of attack of the monoplane for fixed wing area. This means that the elimination of thickness drag for the infinite aspect ratio Busemann biplane is accompanied by a doubling of either the viscous drag or the drag due to lift. If a monoplane at its design operating conditions has a thickness drag greater than the viscous drag of the wing, or greater than the drag due to lift, then the biplane offers a possible drag reduction for the design conditions.

The aerodynamic properties of the Busemann biplane of finite* aspect ratio have been investigated by Sears and Tan [2,3], and the practical application of this arrangement has been studied in detail by George[4]. Preliminary analysis of George's results indicate that the Busemann biplane is inferior to a monoplane for the design operating conditions now contemplated for supersonic aircraft. This is true because the thickness drag of the monoplane wing is not ordinarily great enough to justify its elimination by essentially doubling the viscous drag or drag due to lift.

However, the Busemann biplane is not the only type of biplane which warrants consideration for supersonic use. In this report a preliminary analysis of non-interfering biplanes will be initiated (this was suggested by the airfoil cascades of Chapter III).

*For the rotationally symmetric version of the Busemann biplane see Ref. 5.

3. POTENTIAL ADVANTAGE OF THE NON-INTERFERING BIPLANE

In the overall design of an aircraft, structural and aerodynamic properties must be weighed simultaneously. In the following comparison aerodynamic equivalence is maintained, and the structural properties of the monoplane and biplane are compared.

Consider a monoplane wing of given aspect ratio, wing area and thickness ratio. Compare this with a biplane system having two identical wings each with the same aspect ratio and thickness ratio as the monoplane and each having half the monoplane wing area. If the individual biplane wings are spaced so that there is no interference at the design Mach number, then the biplane system will have the same lift and total drag as the monoplane at the same angle of attack. In this example Reynolds number effects are neglected, and external wing bracing is not considered. The two wing systems are then aerodynamically equivalent at the design Mach number.

For geometrically similar wings the total weight of structural material required for bending and shear is proportional to the total wing volume. The volume of the two biplane wings is $1/\sqrt{2}$ times the volume of the monoplane wing, and a corresponding saving in structural weight is indicated for the biplane. This saving amounts to approximately 29% of the bending and shear material in the monoplane wing. (Greater savings would be obtained for triplanes, quadriplanes, etc.) The structural material which depends on wing area would have the same weight for both wing systems; hence the percent saving on total wing weight would be somewhat less than 29%.

The above comparison suggests a potential advantage for the non-interfering biplane, this advantage being essentially the result of a scale effect. In comparing the non-interfering biplane with the Busemann biplane two differences should be noted. The potential advantage of the non-interfering biplane applies at and above the design Mach number. For the Busemann biplane the potential advantage was confined to the design Mach number. The non-interfering biplane retains its potential advantage for high and low aspect ratios. The Busemann biplane principle is confined essentially to high aspect ratios. (It will be shown later that the non-interfering biplane may, for practical reasons, be better suited to the low aspect ratio range.)

4. UNEQUAL DISTRIBUTION OF LIFT BETWEEN BIPLANE WINGS

At supersonic Mach numbers below the design value, and at all subsonic speeds there will be interference between the two biplane wings. As a result of this interference the equal distribution of lift between the two wings, present in the design condition, may be lost. In the extreme case of infinite aspect ratio staggered rectangular wings, having the same incidence, the lift transfer is complete at some Mach number between unity and the design value, so that all of the lift is carried on one wing. (A related problem arises for the Busemann biplane.[4]) Designing the wing structure for this condition would eliminate all of the potential advantage of the biplane arrangement; hence this is one of the major problems to be solved. (For a missile launched from a supersonic aircraft this problem might not arise.)

If the aircraft, or missile, operated under the above unfavorable interference conditions for a very small fraction of its flight time, it might be justifiable to accept reduced safety factors. The probability of encountering destructive gusts, for example, while in the interference condition would be reduced in proportion to the time interval.

If the time spent operating in the interference condition is not sufficiently small to justify reduced safety factors, then two different design philosophies may be considered.

The first possibility is to design the biplane wing system for the minimum possible lift transfer. This suggests using low aspect ratio wings, and possibly dissimilar planforms for the upper and lower

wings. Both of these trends should tend to eliminate the complete lift transfer which may occur for the infinite aspect ratio rectangular wing system. (The ratio of gap to span should be a major parameter here.)

The second possibility is to connect the wings by external struts and so distribute the load more evenly between them. This of course involves additional drag for the struts and some additional weight. An aerodynamically cleaner arrangement would be the "pyramid" type biplane illustrated. The simultaneous taper of chord and gap would result in a non-interfering biplane at the design Mach number.

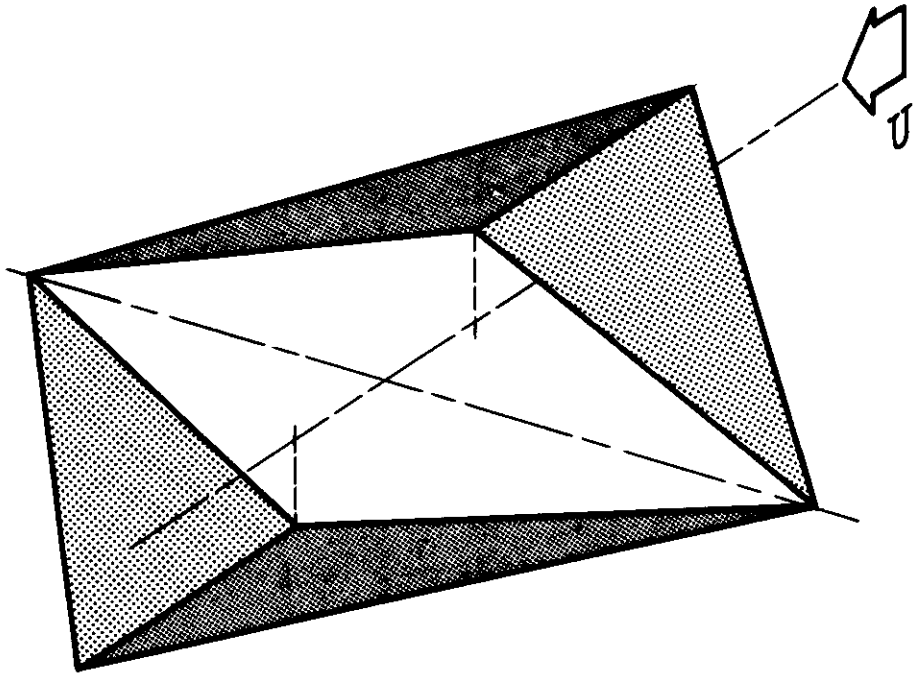

Comparing the first and second procedures, the design of low aspect ratio dissimilar wings for the biplane has the advantage of tending to eliminate the lift transfer trouble at its source. This means that another unfavorable consequence of the lift transfer, the corresponding increase of vortex drag, would be avoided. Another point in favor of the low aspect ratio wings is that they are structurally efficient.

The second procedure, especially as represented by the pyramid type wing, has the fundamental advantage of making use structurally of the overall depth of the wing system. This overall depth is not utilized structurally in the cantilever type biplane.

Another possibility for the reduction or elimination of lift transfer between the biplane wings is the use of movable wings or the use of aero-elastic wing properties. However, these methods seem less desirable than the procedures previously discussed.

5. OPERATION AT LOW SUBSONIC SPEEDS

The aerodynamic equivalence of the monoplane and non-interfering biplane exists at and above the design Mach number. Below the design Mach number the interference of the two biplane wings generally results in aerodynamic inferiority for the biplane.

There is very little information available on the subsonic characteristics of the particular biplane arrangements that seem desirable for supersonic operation. However, the characteristics of a low aspect ratio rectangular wing biplane are available and are of some interest.

In the following comparison the biplane wings are assumed to have no stagger or twist, and both wings are at the same incidence. For an aspect ratio of 3 and a gap/chord ratio of 1 the biplane has a vortex drag (induced drag) 1/3 greater[6] than the geometrically similar monoplane having the same total wing area. (Increasing the gap/span ratio would reduce the vortex drag for the biplane.) Such a drag increase would involve an appreciable performance reduction for the biplane. The importance of this would depend (to some extent) on the fraction of total flight time spent in subsonic operation.

The biplane would also have a lower $\frac{dC_L}{d\alpha}$ than the monoplane by about 20%[6] and probably a reduction in $C_{L_{max}}$ also [7]. The order of magnitude of this reduction might be 5 or 10% (this is uncertain). Both $C_{L_{max}}$ and $\frac{dC_L}{d\alpha}$ presumably could be improved by further separating the biplane wings, since in the limiting case of infinite separation the system must behave as two non-interfering monoplanes.

6. STABILITY AND CONTROL

In addition to the problems already discussed there will probably be new stability and control problems requiring investigation for the biplane arrangement. These problems might arise from alteration of the downwash field (compared to that produced by a monoplane), from the lift transfer between the biplane wings, and possibly from the reduction of span (compared to the monoplane).

However, no attempt will be made to investigate such problems here since they can be studied more easily for specific configurations.

7. CONCLUSIONS

1. It is tentatively concluded (largely from the results of Ref. 4) that the Busemann biplane does not offer any obvious improvements over a monoplane arrangement for the design conditions now contemplated for supersonic aircraft.
2. An inherent structural advantage of non-interfering supersonic biplanes as compared to aerodynamically equivalent monoplanes appears as the result of a scale effect for geometrically similar structures.
3. One possible disadvantage of the non-interfering biplane is the transfer of lift from one wing to the other which may occur below the design Mach number. A second disadvantage is the reduction in subsonic performance (compared to a monoplane).
4. Further investigation of non-interfering supersonic biplanes is warranted, especially when subsonic performance is relatively unimportant. (Subsonic performance might be completely unimportant for a supersonic missile launched from a supersonic aircraft.)
5. Low aspect ratio biplanes (possibly having connected upper and lower wing tips) are suggested for more detailed study.
6. More information will be needed on the subsonic and supersonic aerodynamic characteristics of low aspect ratio biplane arrangements.

8. REFERENCES

1. Busemann, A.: "Aerodynamischer Auftrieb bei Uberschallgeschwindigheit," Luftfahrtforschung 12, pp 210-220, 1935.

2. Sears, W. R. and Tan, H. S.: "The Aerodynamics of Supersonic Biplanes," Quarterly of Applied Mathematics, Vol. 9, No. 1, April, 1951.

3. Tan, H. S.: "The Aerodynamics of Supersonic Biplanes of Finite Span," WADC Technical Report 52-276, December, 1950.

4. George, M. B. T.: "Investigation of the Supersonic-Biplane Configuration," Graduate School of Aeronautical Engineering, Cornell University, May, 1952.

5. Ferri, A.: "Application of the Method of Characteristics to Supersonic Rotational Flow," NACA TR 841, 1946.

6. Glauert, H.: "The Elements of Aerofoil and Airscrew Theory," University Press, Cambridge, 1926.

7. Diehl, W. S.: "Engineering Aerodynamics," Ronald Press Co., New York, 1936.

APPENDIX IV-A

STRUCTURAL WEIGHT COMPARISON BETWEEN A MONOPLANE AND AN "EQUIVALENT" BIPLANE

The example considered in Section 3 is discussed in more detail here. A monoplane with a given wing area S and arbitrary planform is replaced by a biplane in which each wing of area S/2 is geometrically similar to the monoplane wing as shown below. At the same angle of attack each wing system will have the same total lift L and drag D.

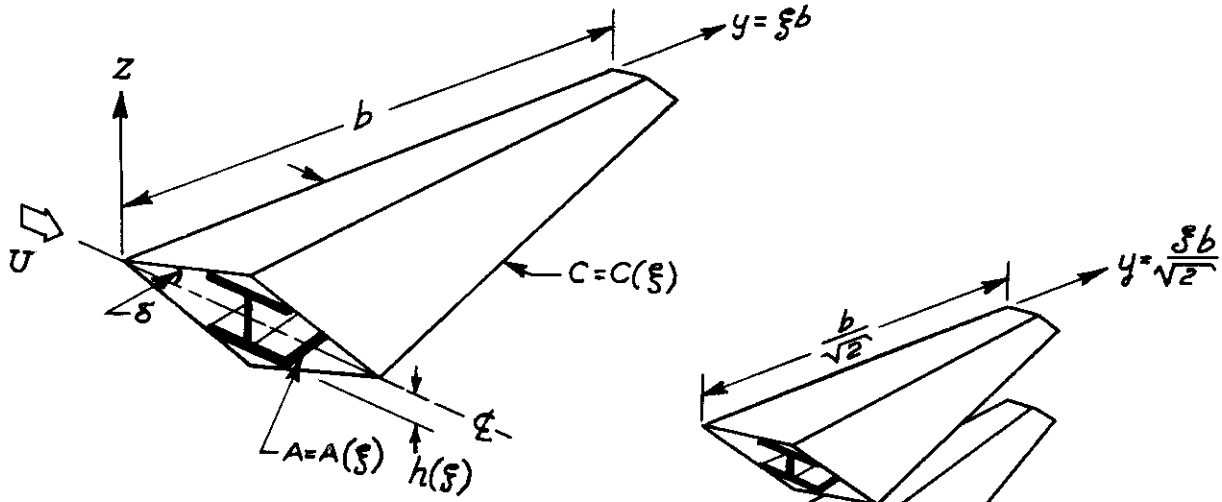

Not only are the wing shapes similar, but so also are the supporting structures (spars). Thus, at each non-dimensional spanwise station $\xi = y/y_{max}$, the cross-sectional area of the monoplane structure is $A(\xi)$ while that of each biplane wing is $\frac{1}{2} A(\xi)$. Because of the geometric similarity the corresponding lift distributions will also be similar;

on the monoplane wing the lift per unit span is $\ell_m = \ell(\xi)$ while on each biplane wing $\ell_b = \frac{1}{\sqrt{2}}\ell(\xi)$; $L = b\int_0^1 \ell(\xi)d\xi$. For the monoplane, the shear stress at the spanwise station $y_m = \xi_1 b$ is

$$s.s._m = \frac{1}{A_m(y_m)}\int_{y_m}^{b} \ell_m(y)dy = \frac{b}{A(\xi_1)}\int_{\xi_1}^{1} \ell(\xi)d\xi$$

while that of each biplane wing at $y_b = \xi_1 b/\sqrt{2}$ is

$$s.s._b = \frac{1}{A_b(y_b)}\int_{y_b}^{\frac{b}{\sqrt{2}}} \ell_b(y)dy = \frac{b}{A(\xi_1)}\int_{\xi_1}^{1} \ell(\xi)d\xi$$

Thus both wing systems exhibit the same shear stress throughout.

The maximum bending stress at each station is $b.s. = Mz_{max}/I$, where M is the bending moment, z_{max} the half-depth and I the moment of inertia of the spar cross-section. By geometric similarity $I_m = 4I_b$. The bending moment for the monoplane at the spanwise station y_m is

$$M_m = \int_{y_m}^{b}(y-y_m)\ell_m(y)dy = b^2\int_{\xi_1}^{1}(\xi-\xi_1)\ell(\xi)d\xi$$

and for the biplane at y_b

$$M_b = \int_{y_b}^{\frac{b}{\sqrt{2}}}(y-y_b)\ell_b(y)dy = \frac{b^2}{2\sqrt{2}}\int_{\xi_1}^{1}(\xi-\xi_1)\ell(\xi)d\xi$$

Thus

$$b.s._m = \frac{M_m h}{I_m} = \frac{hb^2}{I_m}\int_{\xi_1}^{1}(\xi-\xi_1)\ell(\xi)d\xi = b.s._b$$

and the bending stresses are equivalent. The bending deflections can be shown to be geometrically similar, also.

The final comparison relates the weight of structural material required for bending and shear in each of the two systems. For the monoplane

$$W_m = \int_0^b A_m(y)\rho(y)\,dy = b\int_0^1 A(\zeta)\rho(\zeta)\,d\zeta$$

where W is the structural weight and ρ the specific weight of the material. For the biplane

$$W_b = 2\int_0^{\frac{b}{\sqrt{2}}} A_b(y)\rho(y)\,dy = \frac{W_m}{\sqrt{2}}$$

Thus the biplane will effect a saving in structural weight.

CHAPTER V

SURVEY OF PRESENT STATUS

SUGGESTIONS FOR FURTHER RESEARCH

1. PLANAR SYSTEMS

Study of the results for planar wings shows that substantial drag reductions, through the use of spanwise distribution of camber, may be achieved only for low reduced aspect ratios. Fig. 1 summarizes the improvements resulting from camber and twist distributions. With rectangular wings the best camber distributions found here gave increases in C_L^2/C_D of 16.7% for an AR = 1, 2.8% for an AR = 2, and only 1.2% for an AR = 4. These are the improvements in C_L^2/C_D over that of a flat wing with the same planform. Although the camber distribution found was not the absolute optimum, still it is not to be expected that much improvement in C_L^2/C_D remains. For the diamond planform wing of aspect ratio* two it was calculated that C_L^2/C_D could be improved 18.1% over the flat plate value.

*Here the aspect ratio has been computed by the conventional formula AR = (span)^2/area. The concept so defined loses its significance for planforms which deviate markedly from the rectangular shape. If, instead, the aspect ratio is defined as (area)/(chord)^2 the value remains the same for the rectangular wing but becomes 1/2 for the diamond wing. This shows that "low aspect ratio" is a relative concept. In the present context "low" might be taken to mean near unity or lower for rectangular wings and near two or lower for diamond wings. It is interesting to note that the aspect ratio defined both ways appears in the formula for the drag of slender wings with elliptical chordwise and spanwise loadings"

$$\frac{C_D}{C_L^2} = \frac{1}{\pi\left(\frac{SPAN^2}{AREA}\right)} + \frac{M^2-1}{2\pi}\left(\frac{AREA}{CHORD^2}\right)$$

(Jones, R. T., "The Minimum Drag of Thin Wings in Frictionless Flow", Jour. Aero. Sci. Vol. 18, No. 2, Feb. 1951.)

SUMMARY OF CALCULATED IMPROVEMENT IN C_L^2/C_D RESULTING FROM TWIST AND CAMBER FOR SEVERAL PLANFORMS

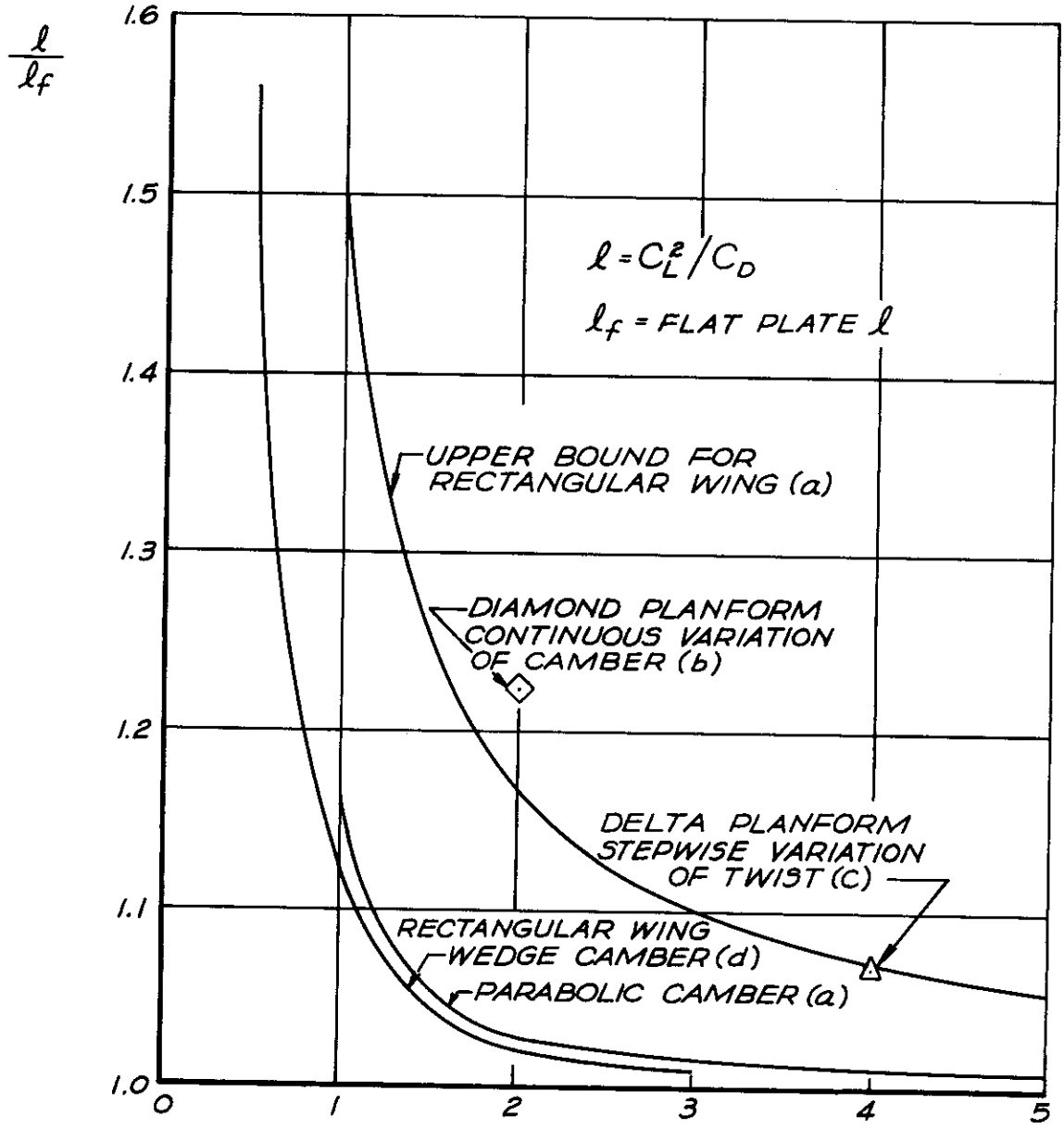

(a) SEE CHAPTER II, SECTION 5

(b) SEE CHAPTER II, SECTION 4

(c) SEE REF. 6 OF CHAPTER II

(d) SEE REF. 5 OF CHAPTER II

FIGURE 1

Thus, noticeable drag reductions can be achieved for low reduced aspect ratios. For flight at maximum L/D the improvement in C_L^2/C_D for $AR_{\square} = 1$ or $AR_{\diamond} = 2$ corresponds* roughly to an 8% reduction in drag. By the analysis given in Chapter I this would lead to nearly a 25% increase in payload.

The reduced aspect ratio, AR_r, referred to above is related to the geometric aspect ratio at any arbitrary supersonic Mach number by the formula $AR_r = \sqrt{M^2 - 1}\, AR$. The calculations were carried out for the Mach number at which the reduced and geometric aspect ratios are identical, $M = \sqrt{2}$.

The examples considered illustrate the cases in which the camber distributions are affected by taper exclusively (diamond wings) and by finite tips exclusively (rectangular wings).

The results obtained indicate the desirability of shaping low aspect ratio wings to decrease the drag due to lift. Wing alone results, however, are to be regarded as incomplete for practical design purposes. Such results do show qualitatively the nature of the drag saving to be expected, and the methods developed should prove a valuable starting point for the study of more complex cases. Whenever the reduced aspect ratio is small, the pressure distribution on a wing attached to a fuselage is strongly affected by the upwash field around the fuselage. Beane** has studied

*For the most part in this report C_D refers to the sum of wave and vortex drag only. It is easy to show that at $(L/D)_{max}$

$$\frac{dD_t}{D_t} = -\frac{1}{2}\,\frac{d(C_L^2/C_D)}{C_L^2/C_D}$$

where the total drag, D_t, includes the parasite drag.

**Beane, Beverly J., "The Effect of Planform on the Lift to Drag Ratio of Wing-Body Combinations at Supersonic Speeds," Douglas Aircraft Company Report No. SM-14454, July 1952.

the influence of the fuselage upwash field on the lift of flat plate wings of various planforms. It follows from the calculations made there that it is necessary to account for fuselage interference in order to obtain the optimal shaping of a low aspect ratio wing attached to a fuselage. Future study should be directed toward combining this work with that of the present report.

The effect of wing incidence should be included in the study of wing and fuselages in combination. The drag due to lift of the fuselage also should be taken into account. An example illustrative of the necessity for considering the entire wing-fuselage combination in evaluating lift and drag due to lift is that of a wing at zero angle of attack attached to a fuselage which is at positive angle of attack. Under such circumstances a flat plate wing will carry lift but no drag. The drag penalty, of course, will appear as drag due to lift of the fuselage.

2. SPATIAL LIFT DISTRIBUTIONS

The study of spatial lift distributions is still in an early stage, and it is perhaps most important to list briefly the problems yet to be solved.

In proceeding from the study of planar lift distributions to the study of spatial distributions three new factors are encountered. First, the lift and thickness effects are not completely separable as they were in the planar case, since in spatial distributions an interference drag term appears. Second, the introduction of side forces is possible, as in the case of "ring" wings, and interference may exist between lift and side force. Third, for lifting elements alone the optimum distribution in a given space is not generally unique, there being a family of lift distributions each member of which produces the same minimum of wave plus vortex drag. (For planar distributions the optimum is generally unique).

Each of the above factors suggests problems for further research, some of which are currently being studied. The investigation of spatial thickness distributions and their interference with lift distributions has been initiated. The interference between side force and lift should be studied to determine under what circumstances this interference disappears and separable problems result. Also the non-uniqueness of optimum lift distributions raises the problem of determining which member of the optimum family has the least wing area or is best suited for structure.

Perhaps the biggest problem is the approximation of theoretically optimum lift distributions by practicable wing systems. However, the theoretical optimum should at least serve as a useful guide in practical design.

3. BIPLANE LIFT DISTRIBUTIONS

For non-interfering biplanes, as compared to aerodynamically equivalent monoplanes, a potential structural advantage has been shown. This advantage is the result of a scale effect for geometrically similar structures.

Further research is required to determine whether or not this potential advantage can be realized in practice. The possible transfer of lift between the wings of the biplane at Mach numbers below the design value should be studied. It is desirable to find a biplane configuration which produces an even distribution of lift between the wings for all flight conditions.

At subsonic speeds the performance of the biplane is inferior to that of the monoplane. Design studies are necessary to determine whether or not the subsonic performance is a critical factor in the design.

It is recommended that further studies be made on low aspect ratio biplane wing arrangements in an effort to solve the problems mentioned and those which may arise in stability and control.